2016

Isolation Of Epicardial Cells From The Cover Of The Heart For Assessment Of Running Exercise-Induced Gene Expression

Laura Solomon
University of Vermont

ISOLATION OF EPICARDIAL CELLS FROM THE COVER OF THE HEART FOR ASSESSMENT OF RUNNING EXERCISE-INDUCED GENE EXPRESSION

A Thesis Presented

by

Laura Solomon

to

The Faculty of the Graduate College

of

The University of Vermont

In Partial Fulfillment of the Requirements
for the Degree of Master of Science
Specializing in Cellular, Molecular, and Biomedical Sciences

May, 2016

Defense Date: March 28, 2016
Thesis Examination Committee:

Jeffrey L. Spees, Ph.D., Advisor
Tamara Williams, Ph.D., Chairperson
Matthew Poynter, Ph.D.
Cynthia J. Forehand, Ph.D., Dean of the Graduate College

ABSTRACT

The cover of the heart, or epicardium, consists of a single layer of mesothelial cells. During cardiac development, epicardial cells undergo Epithelial-to-Mesenchymal Transition (EMT) to form multipotent precursors known as epicardial-derived cells (EPDC). The EPDC migrate into myocardial tissue (containing cardiomyocytes) and subsequently differentiate into fibroblasts, myofibroblasts, and smooth muscle cells. In adult hearts, a similar process of epicardial cell proliferation, migration, and differentiation occurs after myocardial infarction (MI, heart attack). EPDC differentiation into vascular endothelial cells or cardiomyocytes is rare and not well understood. Recently, we observed that running (exercise) in mice promotes differentiation of EPDC into microvascular endothelial cells (CD31+). After running, EPDC appear to generate endothelial cells and not other cardiac cell types. Of interest, running promotes cardiac hypertrophy that requires additional perfusion (blood flow) and may therefore stimulate the contribution of EPDC to capillaries. We hypothesized that running exercise induces gene expression in epicardial cells that promotes endothelial specification. To test our hypothesis, we developed an efficient method to directly isolate primary adult epicardial cells from the heart cover based on their expression of integrin-β4 (CD104). After 2 hours of protease digestion, we used Magnetic-Activated Cell Sorting with antibodies against CD104 (CD104 MACS) to obtain undifferentiated epicardial cells; this was confirmed by expression of Keratin-18, an epicardial-specific protein in the heart. By cDNA microarray assays and bioinformatics analysis, we compared the gene expression profile of epicardial cells isolated from running-conditioned mice with that of age-matched controls (non-runners). Our data suggest that extracellular matrix remodeling in the heart is mediated, in part, by epicardial cells during running. Furthermore, we identify epicardial gene expression for cell signals/pathways and transcription factors that may enhance vascular perfusion after MI through promoting angiogenesis or endothelial specification of epicardial derivatives.

ACKNOWLEDGEMENTS

A graduate student could not find a better team of mentors for a thesis committee. I thank Dr. Tamara Williams for her positivity and ability to inspire genuineness, balance, and empathy in others; Dr. Matthew Poynter for his support during transitory periods and for providing objective, sound advice. I thank my advisor, Dr. Jeffrey Spees, for demonstrating scientific aptitude and creativity and for encouraging his lab members to ask questions, even (especially?) while mapping transcription factor binding sites to ten kilobase promoter regions. Thanks, Jeff, for turning my graduate school experience into gold. Many thanks go to UVM and the Department of Biology for welcoming me to campus a few months early. From Marsh Life Science, I thank Dr. Alicia Ebert for her support from the start, guidance, and wisdom; Ashley Waldron for her honest opinion at the drop of a hat. I thank Dr. Nicholas Heintz, Dr. Christopher Huston, and Ms. Erin Montgomery for providing me with a seamless transition into the CMB program. Nick, thank you for cultivating equality and student growth. Many thanks to my incredible colleagues/friends for all of the late night white-board sessions and for lots of laughs (LOLs); to this end, I thank Blas Guigni, Jessica Sheehe, Miranda Redmond, Phyu Thwe, and Devin Champagne for their precocious wit. I thank Devin for his willingness to brainstorm “the next five” transferrin experiments. I thank Dr. Stephen Everse for listening and for understanding and I thank Dr. Bob Kelm for his profound lectures and his module-based teaching style. I thank the myriad professors who challenged and changed my ways of problem-solving: Drs. Jason Bates, Paula Deming, Alan Howe, Tom Jetton, George Osol, Jason Stumpff, Dave Warshaw, and George Wellman. I greatly appreciate the thought-provoking assignments and exams, all of which were worth the lost hours of sleep and sanity. I thank Dr. Julie Dragon for her insights and expertise. A heartfelt thanks goes to the Spees Lab members, especially to Dr. Aronshtam for his guidance in the business of molecular cloning and for sharing his time and reagents. I thank John McInnis for convincing me to believe in myself one hundred times over, for teaching me about transgenic mice, and for his persistent focus on the science. I thank my

other science friends: Lucas Howard for his academic integrity and for his help with statistical analysis, Perstephanie Hicks for her Prism wizardry and her patience, Suzanne Newberry for her strength and her generous hospitality, and Andrew Perez, who may or may not have ridden a bicycle through Jeffords Hall, for his sense of comic relief. I thank the undergraduate students who participated during lab sessions and asked "mindful" questions.

"The art of living is neither careless drifting on the one hand nor fearful clinging on the other. It consists in being sensitive to each moment, in regarding it as utterly new and unique, in having the mind open and wholly receptive." – Alan Watts

DEDICATION

This thesis is dedicated to my late granddad, Erskine Solomon. During the five years that we co-existed, I formed memories of his infectious laughter and the uncanny display of porcelain clowns in his cigar-scented home. Overtime, I learned more about his essence through stories regarding his restless nature and inevitable fallibility. Once, while driving through a tunnel under the Baltimore Inner Harbor on I-95, he accidentally dropped two dozen oak logs off the back of his pickup truck, stopping traffic flow like a thrombus in the LAD artery. If the stories are true, then it is worth expressing sincere gratitude to him for a quarter of my genome. He would be excited about this research.

TABLE OF CONTENTS

Page

LIST OF TABLES

Table Page

LIST OF FIGURES

Figure Page

CHAPTER 1: INTRODUCTION

1.1. Project relevance to cardiovascular disease

Myocardial Infarction (MI, heart attack) is a sudden and sometimes fatal occlusion of blood flow and nutrient exchange within the myocardium. The inadequate nutrient exchange and oxygen supply between the cardiac vasculature and cardiomyocytes (i.e., cardiac muscle cells) results in local cell death and tissue necrosis (White et al. 2014). The size of the resulting infarct and patient prognosis depend on several parameters such as time to revascularization and degree of reperfusion achieved upon recanalization of the occluded blood vessel.

A leading cause of death, MI affects one in four individuals worldwide (Mozaffarian et al. 2016). In 2015, approximately 735,000 people suffered a heart attack in the United States (Mozaffarian et al. 2016). Current hospital interventions to treat MI promote reperfusion to the area of infarct by chemical removal of the clot (a.k.a. thrombolysis), or through mechanical means such as stenting (NIH: National Heart, Lung, and Blood Institute available online, updated Nov. 2016; Pasotti, Prati, & Arbustini, 2006). Depending on the extent of damage to the heart, cardiac function may continue to decline, even when the thrombus has been successfully removed.

MI results in widespread changes in cellular communication. In tissue with infarction, soluble signaling molecules such as growth factors, cytokines, chemokines, and other chemical mediators (e.g., adenosine triphosphate [ATP], reactive oxygen species, nitric oxide) are released from cardiac myocytes, vascular cells, fibroblasts, and immune cells that elicit responses from various other cell types, including epicardial cells

(Murphy & Steenbergen 2008; Cochain et al. 2013; Horckmans et al. 2016). In the days that follow MI, interstitial fibroblasts, including those that derive from epicardial cells (for details, see below), secrete extracellular matrix to form scar tissue in the necrotic zone (Shinde & Frangogiannis 2014). Although it may eventually lead to cardiac stiffening with potential to promote cardiac failure, in the short-term, cardiac scar formation prevents ventricular rupture and death.

1.2 Background to epicardial and cardiac cell biology

The heart is comprised of cardiomyocytes, interstitial fibroblasts, neurons (Purkinje cells), and a complex, interweaving vasculature comprised of endothelial cells, smooth muscle cells, adventitial fibroblasts, and pericytes (Xin et al. 2013). The heart also contains endocardial cells that form its inner lining, and epicardial cells, that cover its surface. The unique phenotype and function(s) of each cardiac cell type results, in part, from cell signaling, gene transcription and protein expression established during development. For example, growth factors (e.g., BMPs, Wnt/β-catenin, FGFs, Activin/Nodal) direct cardiac myocyte specification during development by activating specific networks of genes that encode transcription factors such as Nkx 2.5, Isl-1, Tbx5, and the receptor, Flk-1 (Später et al. 2014; Olson 2006). To maintain cellular phenotype in adults, genes/proteins for some transcription factors and receptors continue to be expressed (e.g., Gata4) (Evans et al. 2010). Cell-cell communication plays an essential role in relaying information about the physiologic or pathophysiologic state of the heart and other organs. These signals, in turn, influence cardiac function. Other cell types that affect

cardiac function through signaling include immune cells and innervating neural cells (Xin et al. 2013).

During development, the cells that comprise the pro-epicardial organ form the "epicardium", or outer-most layer of the heart (Pérez-Pomares & Muñoz-Chápuli 2002; Reese et al. 2002). Epicardial cells undergo epithelial-to-mesenchymal transformation (EMT), migrating into the heart to produce epicardial derivatives: vascular smooth muscle cells, myofibroblasts, and perivascular fibroblasts that contribute to the formation of the capillary plexus, a vascular network that includes the coronary arteries (Dettman et al. 1998; Reese et al. 2002). During this process, simultaneous changes in EMT-associated transcription factors, migration machinery, cytoskeletal architecture and ECM composition allow epithelial-like epicardial cells to adopt a more mesenchymal, migratory phenotype (Cano et al. 2000; Männer et al. 2001; Thiery et al. 2009)

The adult epicardium is formed by mesothelial cells that do not usually undergo EMT and that remain on the heart surface. This single cell layer is adherent to the subepicardial extracellular matrix and surrounded by pericardial fluid, a lubricant that reduces friction for the heart as it beats within the pericardial sac. The expression of transcription factors (e.g. Tbx18, Wt-1) and cytoskeletal proteins (e.g. Keratin-18) is used to identify epicardial cells (Thorey et al. 1993; Zeng et al. 2011). Adult epicardial cells are typically quiescent but retain their competence for EMT and migration (Figure 1). As such, they have recently have been identified as an important source of cells for cardiac regeneration after injury (Masters & Riley 2014). During MI, the fetal epicardial program is "re-activated," inducing epicardial cells to lose apical-basal polarity and undergo EMT

to form multipotent progenitor cells, called epicardial-derived cells (EPDC) (Zhou et al. 2011; von Gise & Pu 2012). After MI, EPDC migrate through the subepicardium toward areas of infarction (Smart et al. 2013), contributing to the population of cardiac fibroblasts, smooth muscle cells, and to a much lesser extent cardiomyocytes and endothelial cells (Reviewed in Wessels & Pérez-Pomares 2004)

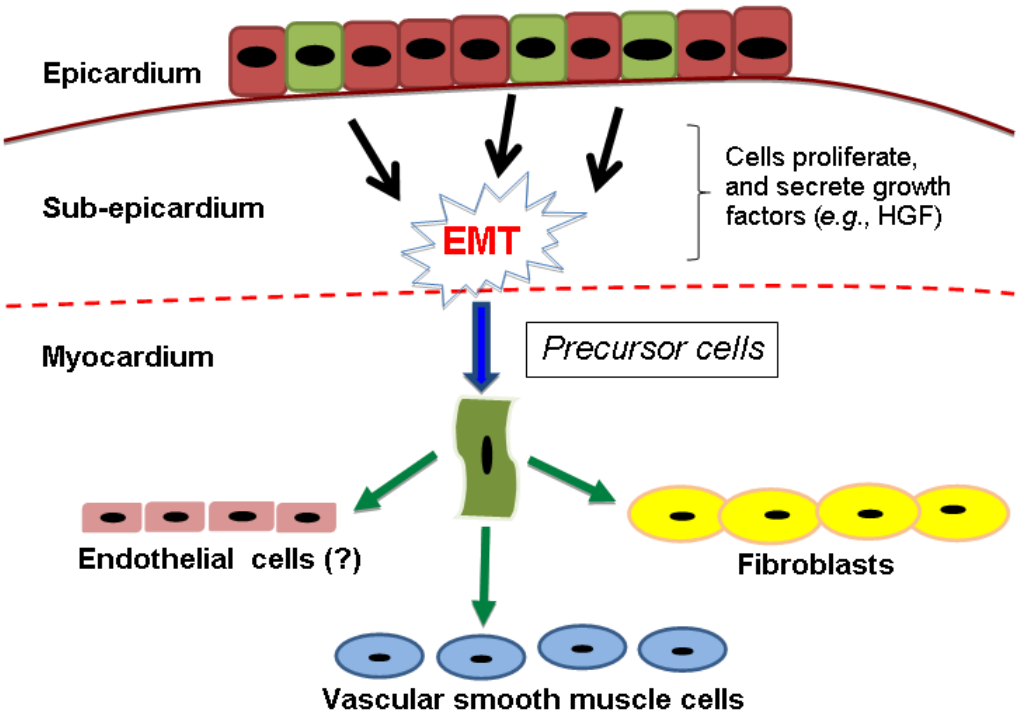

Figure 1. Diagram of epicardial cell layer involved in differentiation. After EMT, precursor cells migrate through the subepicardium and into the myocardium where they may differentiate in various cardiac cell types. EMT= Epithelial-to-Mesenchymal Transition.

In recent work, the Spees Lab developed tools and methods to prime cardiac stem/progenitor cells (CPCs), including EPDC, for delivery to subepicardial sites in order to promote graft success after MI. Importantly, we found that priming cells in a defined combination of C-terminal (4^{th} domain) peptide of Connective Tissue Growth Factor (CTGF-D4) and Insulin supported the survival of grafted cells and also their migration into cardiac tissue with necrosis (Iso et al. 2014) (Rao et al., under review). We hypothesize that this system can be utilized to promote neovascularization and improve cardiac regeneration and function after MI.

1.3 Neovascularization is observed after running exercise, but not myocardial infarction

To better understand the role of the adult epicardium in angiogenesis and vascular preservation/repair after cardiac injury, we are also studying the cell biology of healthy hearts using a mouse model of running-exercise, focusing on the changes that occur in epicardial cells. In adults, running-exercise promotes compensatory changes that improve cardiac performance (function); these changes can contribute to a healthy cardiovascular system and reduce the incidence of cardiovascular disease. Similar to the case for humans and other mammals, running-exercise in mice increases VEGF production and promotes neovascularization that enhances vascular perfusion to support cardiac hypertrophy (i.e., muscle growth) (Asahara et al. 1999; Kehat & Molkentin 2010). In preliminary studies, we found that running-exercise induced epicardial EMT and the differentiation of EPDC

derivatives into microvascular $CD31^+$ endothelial cells that contributed to capillary formation (K. S. Rao, PhD dissertation; University of Vermont).

Importantly, identification of the signaling mechanisms responsible for the positive changes that occur during running-exercise may help to develop therapeutic approaches to improve cardiac perfusion after ischemic injury. Within this Master's Thesis, I provide the first report of epicardial gene expression that occurs in response to running-exercise. Furthermore, I discuss the transcriptional profiling results in terms of cardiac development, remodeling, and cell signaling. Notably, our data may provide a road map for pro-angiogenic signals and pathways that can potentially be exploited to induce endothelial cell fate from adult epicardial cells and/or EPDC in the context of MI.

Chapter 2: METHODS

2.1 Background

To study changes in epicardial cells during running exercise, we developed a novel method for epicardial cell isolation. Other groups have studied epicardial cells by "explant culture", wherein small pieces of cardiac tissue are physically dissected from the heart cover and allowed to adhere in cell culture for 3 days to 1 week (Kim et al. 2012; Greulich et al. 2012). While the explant approach can yield 10^5-10^6 epicardial cells from a single heart grown in a cell culture dish, it has major disadvantages that may contribute to data artifact(s) and misinterpretation of regulatory mechanisms that operate *in vivo*. In addition to the potential for heterogeneity within the population of isolated cells, the extended time that cells spend in culture is also a problem (i.e., adhered to plastic culture dishes and bathed in serum-containing medium). Culture of primary epicardial cells is well known to induce proliferation and EMT (Described in Lamouille et al. 2014).

The main objective of our study was to identify key differences in epicardial cell gene transcription between mice that engaged in running-exercise over a 1-week period compared with aged-matched (non-running) controls. To minimize transcriptional changes in epicardial cells during the isolation process, we used both chemical and mechanical means to carefully remove epicardial cells from the heart in a rapid and efficient manner. To minimize destruction of cell surface epitopes (e.g., receptors, integrins, etc.) and avoid activation of intracellular signaling cascades, we incubated individual hearts in an enzyme solution that contained concentrated collagenase and dispase, but not other proteases. Moreover, we incubated hearts with low-dose

cyclosporine A to promote cell survival (Jung et al. 2008; Sachewsky et al. 2014). To further optimize this approach, we simultaneously performed mechanical/chemical digest by employing constant, gentle shaking with specialized equipment. Importantly, these methods isolate primary adult epicardial cells from adult mice while reducing contamination by other cell types, including fibroblasts and blood cells.

Previously, we identified an epicardial-specific cell marker for the heart, CD104 (integrin-β4). Expression of CD104 is exclusive to epicardial cells of the heart, as demonstrated by immunohistochemistry of cardiac tissue sections and by immunofluorescence staining of isolated cells after enrichment by Fluorescent-Activated cell Sorting (FACS) (Rao, et al., under review). Accordingly, we took advantage of the specificity of CD104, and performed Magnetic-Activated Cell Sorting (CD104 MACS) to further enrich epicardial cells. Subsequently, we confirmed this result by staining cells isolated by CD104 MACS with antisera against Keratin-18, a specific marker of epicardial cells in the heart (Rao et. al., PhD dissertation; University of Vermont). To our surprise, we found that the majority of cells isolated by our initial chemical/mechanical digest method were Keratin-18^{+}, even before sorting. By CD104 MACS, we were able to increase the number of Keratin-18^{+} cells obtained, indicating further enrichment for native epicardial cells in the population. Applying our isolation method, and CD104 MACS, we then isolated total RNA from primary epicardial cells of runners and non-runners and generated transcriptional profiles using cDNA microarrays (Figure 2).

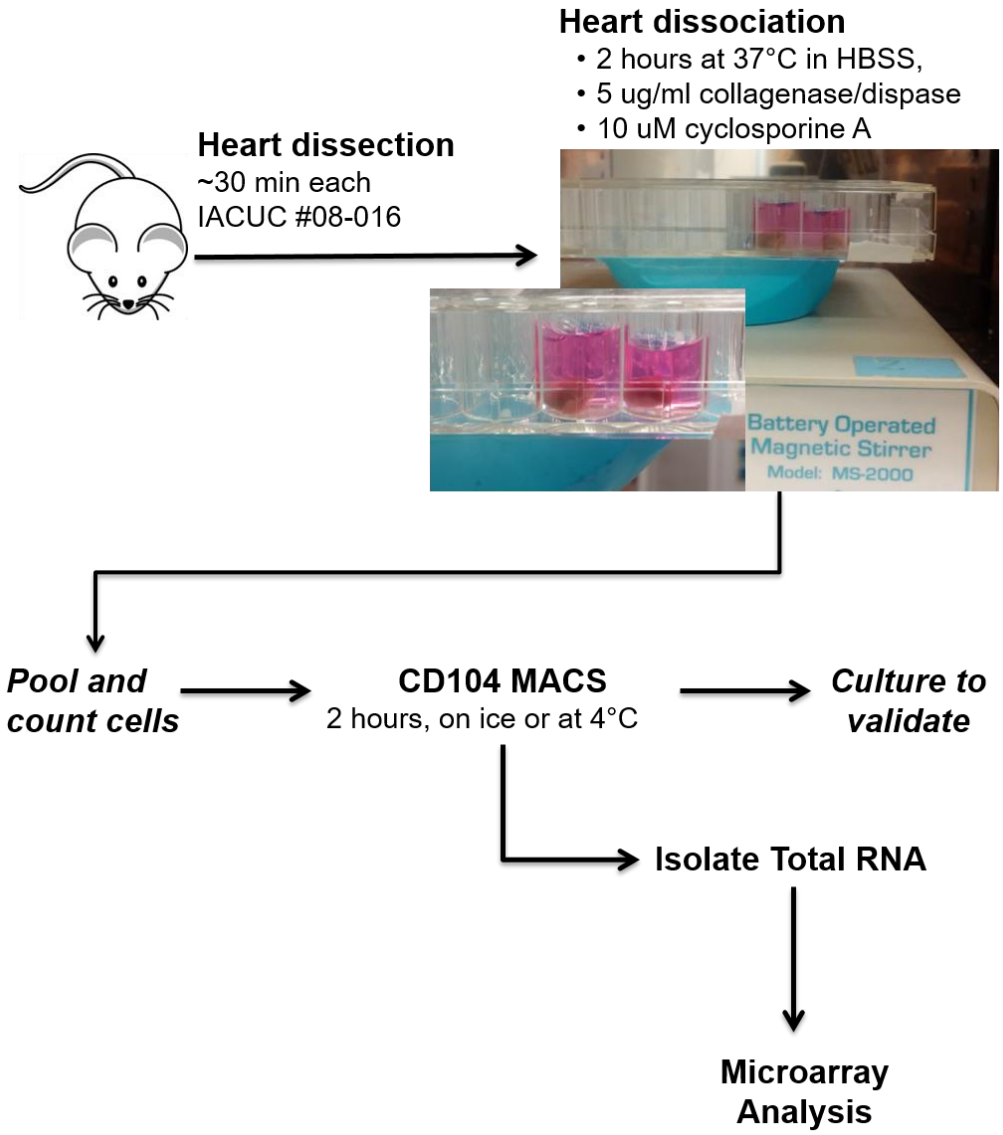

Figure 2. Schematic overview of heart digest and epicardial cell isolation method. N = 5 mice (C57BL/6J, males, 10-weeks of age) per group, housed either with or without a running wheel and odometer. Cell culture incubator was maintained at 37°C, 5% O_2 See Methods for details.

2.2 Running exercise in adult mice

C57BL/6J mice (males, 10 weeks of age; from The Jackson Laboratory, Bar Harbor, ME) were allowed to run ad libitum for 1 week before euthanization and heart harvest. Experimental mice (n = 10 total) were housed individually, provided food and water ad libitum. Each mouse cage was equipped with a running wheel and an attached odometer (CatEye America, Boulder, CO), generously provided by Dr. William Falls, Department of Psychology, University of Vermont. Running distances were recorded every 1 to 2 days. Age-matched male control mice (n = 10) were housed and fed similarly, except without running wheels. All animal work was conducted in accordance with a protocol approved by the Institutional Animal Care and Use Committee of the University of Vermont (IACUC protocol 08-016).

2.3 Epicardial cell isolation

2.3.1 Heart dissection

A sterile fume hood was cleansed with 70% ethanol (Sigma-Aldrich) and exposed to UV light for 15 minutes prior to heart dissection. Each mouse was anesthetized by isoflurane inhalation for 2 minutes (4%, to effect) and underwent cervical dislocation before dissection. After placing the mouse in the fume hood, on a pre-sterilized stainless steel container (ventral side facing up), the fur was cleansed with a 70% ethanol wipe and a central incision was made just below the sternum. The skin was cut laterally below the ribs and the sternum was retracted with a hemostat (Fine Science Tools, Foster City, CA) to expose the diaphragm. A medial incision was made in the diaphragm and cut laterally

toward each side to expose the heart. To clear blood cells by trans-cardiac perfusion, approximately twenty (20) ml of 1x Phosphate Buffered Saline (PBS; Corning, Corning, NY) was injected into the left ventricle (clearance of blood indicated by a blanching change in color in the lungs and liver). The aorta and large vessels were cut and the heart was removed and immediately rinsed with 1x PBS at room temperature (to remove excess blood). The heart was transferred to a solution containing 1x Hank's Balanced Salt Solution (HBSS; Sigma-Aldrich, St. Louis, MO) and maintained at room temperature for no more than 15 minutes. Individual hearts were then transferred into the wells of tissue culture plates that contained the solution for enzymatic digestion.

2.3.2 Enzymatic digestion of the heart cover with collagenase/dispase

Digest solution was freshly prepared on the day of isolation and kept on ice. It consisted of HBSS supplemented with 5 μg/ml Collagenase/Dispase (Roche Diagnostics GmbH, Mannheim, Germany) and 10 μM Cyclosporine A (Cayman Chemical Company, Ann Arbor, Michigan). Hearts were placed into individual wells of a 24-well plate (Fisher, Pittsburg, PA) and fully submerged into 1 ml of digest solution. The plate was taped to a plastic weigh boat containing a magnetic stir bar, placed on a battery-operated magnetic stirrer (Elmco Engineering, Rockville, MD) and then transferred to an incubator that was maintained at 37°C and 5% CO_2 for 2 hours.

2.3.3 CD104 Magnetic-Activated Cell Sorting (CD104 MACS).

Isolated cells from individual hearts were pooled according to experimental group (running versus non-running). Cells were collected into 50 ml conical tubes (Falcon). Hearts were washed twice in 1x PBS and cells were collected. Cells were centrifuged at 800 x g for 8 minutes at 22°C, carefully triturated with a glass Pasteur pipette, and gently re-suspended in 500 µL of MACS buffer. MACS buffer was prepared as α-Minimum Essential Medium (MEM, Sigma) supplemented with 2 mM EDTA (Sigma-Aldrich) and 0.5% Biotin-free BSA (Sigma). Immediately after re-suspension in 500 µl MACS buffer, cells were incubated with rat anti-mouse CD104 antibody (1:100, MCA2369; AbDSerotec, Raleigh, NC) for 30 minutes on ice, with gentle agitation every five minutes. After incubation, cells were gently washed with 30 ml MACS buffer and mixed by inversion. Cells were centrifuged at 800 x g for 8 minutes, re-suspended in 800 µl of MACS buffer, and 200 µl of anti-rat IgG microbeads (Miltenyi, San Diego, CA) was added to the solution. Cells were incubated on ice for another 30 minutes, with gentle agitation every 5 minutes, and then washed with 30 ml of MACS buffer before centrifugation at 800 x g for 8 minutes. LS-Columns (Miltenyi Biotech, Bergisch Gladbach, Germany) were placed onto a QuadroMACS Separator (Miltenyi Biotech) at 4°C for 10 minutes prior to use. Columns were equilibrated with 5 ml MACS buffer and cells were re-suspended in 5 mL MACS buffer and placed onto the column. Cells labeled with MACS Microbeads were held in suspension within the column by the MACS Separator magnetic field and released after three washes with MACS buffer. Cells were eluted from the column in 5 ml MACS buffer. The CD104-positive fraction was collected

in a sterile, separate tube. Cells were centrifuged at 800 x g for 8 minutes, resuspended in MACS buffer, and a cell count was performed by hemocytometer.

2.4 RNA isolation

Total RNA was isolated with the Quick-RNA MicroPrep kit as per the manufacturer's instructions (Zymo Research Corp., Irvine, CA). Briefly, cells were re-suspended in 100 µl RNA Lysis Buffer and vortexed for 2 seconds. To the solution, 100 µl of 100% Ethanol was added to the samples and mixed by vortexing. The sample was transferred to a Zymo-Spin IC Column with Collection Tube and centrifuged. All centrifugations took place at 15,000 x g for 30 seconds at room temperature and flow-through was removed after each centrifugation. The samples were immobilized on the column and treated with DNase I for 15 minutes at room temperature and then the column was centrifuged. RNA Prep Buffer was added to the column and then centrifuged for 30 seconds. The sample was washed twice with RNA Wash Buffer and then eluted from the column with DNase/RNase-free water into an RNase-free tube. Sample concentrations were measured with a spectrophotometer at λ= 260/280 nm and 260/230 nm and stored at -80°C before submission to the DNA Core Facility (University of Vermont, Burlington).

2.5 Cell culture, antibodies, and immunocytochemistry

After isolation, cells were plated in α-MEM (Sigma) containing 10% fetal bovine serum (FBS; Gibco/Life Technologies, Grand Island, NY), 10 µM L-glutamine, and 10

μM penicillin/streptomycin (Gibco/Life Technologies, Carlsbad, CA) and then plated on sterile glass coverslips in a 24-well plate (Fisher). Cells were transferred to an incubator that was maintained at 37°C with 5% CO_2 and allowed to adhere for 24 hours before fixation. After a gentle wash with 1x PBS, cells were fixed with cold 4% paraformaldehyde (Miltenyi) for 15 minutes at room temperature. Fresh blocking buffer was prepared in 1x PBS with 0.25% Triton-X 100 and 3% goat serum. Cells were incubated with blocking buffer for 1 hour at room temperature. Rabbit anti-Keratin-18 antibody was prepared in blocking buffer (1:500, Sigma-Aldrich, C-terminal antibody). Cells were incubated with primary antibody overnight at 4°C and then washed thrice with 1 x PBS at room temperature. Goat anti-Rabbit AlexaFluor 594 was prepared in blocking buffer (1:500 vol/vol) and cells were incubated with secondary antibody for 1 hour at room temperature. After 3 washes with 1 x PBS at room temperature, coverslips were mounted with Vectashield containing DAPI (Vector Laboratories, Burlingame, CA) and stored at 4°C until visualization by epi-fluorescence microscopy. Images were captured using a Leica DM600B microscope equipped with a CCD camera (Leica DFC350Fx) and FW4000 software using channels to visualize nuclei at λ= 355 nm and intermediate filaments at λ= 594 nm for 15 ms and 200 ms, respectively. Images were captured at 20x and 40x with PlanApo objectives (Leica).

2.6 Microarray analysis

2.6.1. Running-exercised and control sample microarray

RNA samples were submitted to the UVM Advanced Genome Technologies Core (UVM AGTC). Oligonucleotide microarray analysis of RNA expression levels was performed using the Affymetrix GeneChip, Mouse Gene 2.0 ST (Affymetrix Inc., Santa Clara, CA) according to manufacturer's protocols. In brief, an RNA input of 50 ng was used to generate cDNA through First Strand and Second Strand synthesis reactions (Ovation® Pico WTA System V2, NuGEN). The cDNA samples were then purified using an Agencourt® RNAClean® XP magnetic bead protocol. Following purification, samples were amplified using SPIA reagents (Ovation® Pico WTA System V2, NuGEN). A final cDNA purification was performed (Agencourt® RNAClean® XP). Sample concentrations were determined with 33 μg/mL/A260 constant on a Nanodrop 1000 Spectrophotometer. Approximately 4 μg of cDNA was fragmented and labeled (Encore® Biotin Module, NuGEN). Efficiency of the biotin labeling reaction was verified using NeutrAvidin (10 mg/mL) and a gel-shift assay. Samples were injected into arrays and placed into an Affymetrix Genechip® Hybridization Oven 640 at 45° C and 60 RPM for 16-18 hours. Arrays were stained using the Affymetrix Genechip® Fluidics Station 450 and scanned with the 7G Affymetrix Genechip® Scanner 3000.

2.6.2. Array data analysis

Probe set statistics and identification of differential expression was performed by the Molecular Bioinformatics Shared Resource of the University of Vermont College of Medicine using Partek Genomics Suite® Version 6.6 (Partek Inc., St. Louis, MO).

Probe-level intensities were calculated using the Robust Multichip Average (RMA) algorithm, including background-correction, normalization (quantile), and summarization (median polish), for each probe set and sample. Sample quality was assessed based on 3': 5' ratio, relative log expression (RLE), and normalized unscaled standard error (NUSE). Principal Component Analysis (PCA) was also used to identify outlier samples that would potentially introduce latent variation into the analysis of differential expression across sample groups.

Multivariate Principal Component Analysis was performed on the normalized data set using the covariance matrix. Univariate linear modeling of sample groups was performed by ANOVA. The magnitude of the response (fold-change calculated using the least square mean) and the p-value associated with each probe set and binary comparison were calculated, as well as a "step-up" adjusted p-value for the purpose of controlling false discovery rate (Benjamini, Y, and Y Hochberg, 1995)

Data were analyzed by Gene Set Enrichment (Partek), which uses a right-tailed Fisher's Exact test with a null hypothesis that data are changing together strictly by chance. The alternative is that the data change in concert because they are part of a biological gene set of pathway. Functional clusters and pathways were identified using the DAVID bioinformatics resource (Huang et al. 2009).

Chapter 3: RESULTS

3.1 A combination of protease digestion (collagenase/dispase) and gentle agitation effectively removes epicardial cells from the surface of the adult mouse heart

To obtain primary epicardial cells for gene expression assays, we sought to prospectively isolate cells from the surfaces of adult mouse hearts (C57BL/6J males, 10 weeks old). In preliminary experiments, we attempted a fast (15 minute) digestion approach by incubating hearts in 0.025% trypsin. Isolated primary mouse cells were kept for 24 hours in a minimal medium (α –MEM supplemented with 1% FBS and 10 μM cyclosporine A). Problematically, however, this approach yielded a cell population abundant with spindle-shaped fibroblasts, but that contained few epicardial cells (rounded, epithelial-like morphology) (Fig. 3A).

Instead of using trypsin, we next attempted to incubate whole mouse hearts for 2 hours in a modified saline solution (HBSS) containing collagenase/dispase (5 mg/mL) and 10 μM cyclosporine A. Using this digestion solution, we obtained an average of 15,000 ± 3,100 cells/heart. In contrast to trypsinization, we found that the collagenase/dispase-based digestion method enriched for epithelial-like cells. Some cells adhered in groups (clusters), while others adhered as individual cells. Cells obtained by collagenase/dispase digestion could be maintained in culture for over 1 week (Figs. 3B-D). Notably, in contrast to epicardial explant culture, this method removed epicardial cells directly from the cover of the heart that could be immediately used for isolation of total RNA or protein, or, further enriched by MACS or FACS (see below).

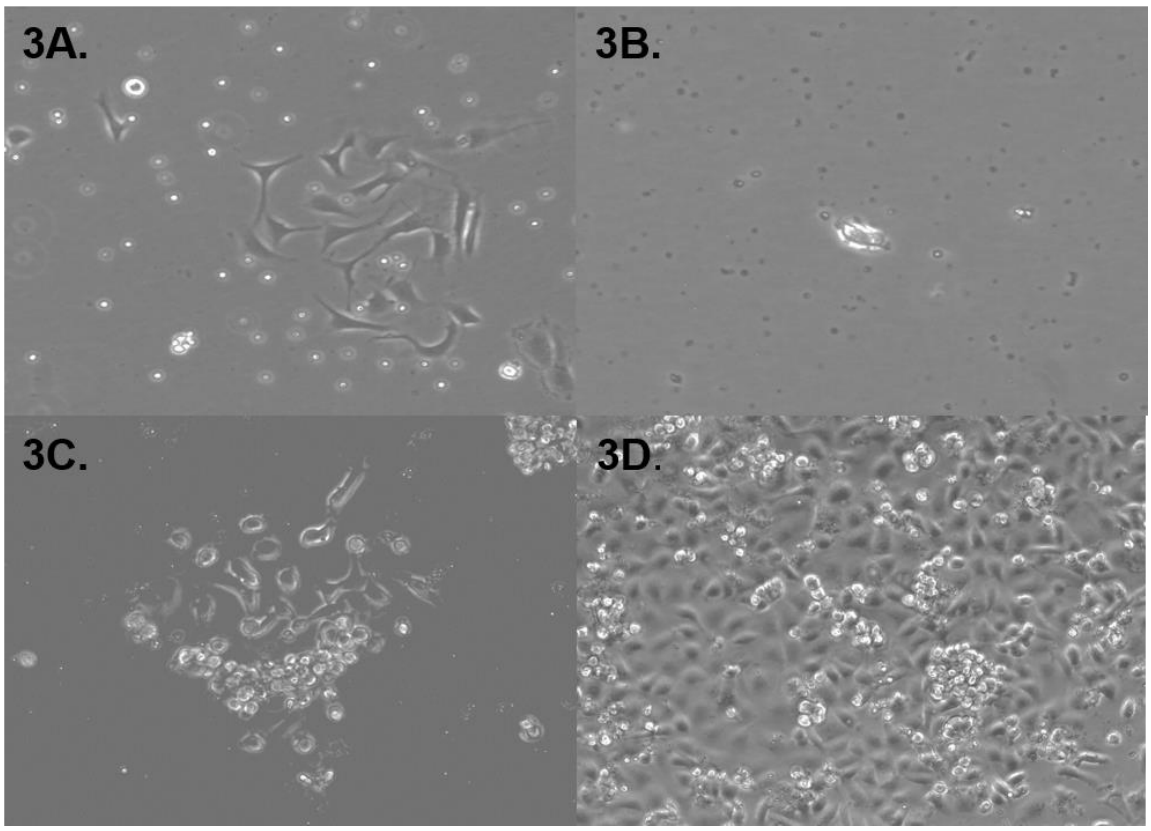

Figure 3. Optimization of heart digest conditions for mouse epicardial cells. (A) Cells cultured for 24-hours after heart digest in 0.025% trypsin at 37°C for 15 minutes. (B) Digest in 50 μg/mL collagenase/dispase yields very few cells. (C) After 2 hour digest with gentle agitation with 5 mg/mL collagenase/dispase, we prospectively isolated primary epicardial cells. (D) One week after digest, epicardial cells with a characteristic cobblestone-like morphology expanded in culture as a single layer and as clusters of cells.

3.2 Isolation of primary adult Keratin-18+ epicardial cells.

After collagenase/dispase digestion, to further enrich for epicardial cells, we immediately sorted cells by MACS. For MACS we used a primary antibody (Rat anti-Mouse CD104) followed by a secondary antibody (Goat-anti Rat IgG) that was conjugated to paramagnetic microbeads. After elution from the MACS column, the resulting cells were cultured for 24 hours, fixed, and permeabilized. We then performed immunofluorescence staining to detect Keratin 18, an epicardial-specific intermediate filament protein in the heart, with an anti-Keratin-18 antibody. Lastly, cells were counterstained with 4',6-diamidino-2-phenylindole (DAPI) to identify cell nuclei. After 24 hours in culture, the number of Keratin$^+$/DAPI$^+$ cells differed significantly between wells containing pre-MACS cells (Fig. 4A), cells from the negative MACS fraction (CD104-negative) (Fig. 4B), and cells from the positive MACS fraction (CD104-positive) (Fig. 4C) (ANOVA, $p < 0.001$, $F = 13.5$).

Surprisingly, even prior to CD104 MACS, most of cell population isolated by collagenase/dispase digestion was Keratin-18$^+$ (82 ± 9 % of total DAPI$^+$ cells). After CD104 MACS, there were additional Keratin-18$^+$ cells (88 ± 10% of total DAPI$^+$ cells) (Table 1), however, CD104 MACS did not significantly increase the number of Keratin-18$^+$ cells (2-tailed t-test, $p = 0.055$). Notably, after 1 week of culture, we did not observe mesenchymal cells, suggesting that the CD104-isolated cells had not undergone EMT (Fig. 4D).

Table 1. Heart digest method selects for epicardial cells and is used to demonstrate gross differences in epicardial cells after running-exercise. An average total cell count (N = 3 experiments, 5 hearts/experiment) is reported for running-conditioned and littermate control mice.

Cell Population	*Keratin-18^{+}: DAPI^{+}*	*Running Exercise*	*Control*
Pre-sort	82 ± 9.9%	57,433 ± 10,500 cells	38,296 ± 7150 cells
Post-sort (CD104^{+})	88 ± 10.2%	39,533 ± 1750 cells	21,778 ± 6500 cells

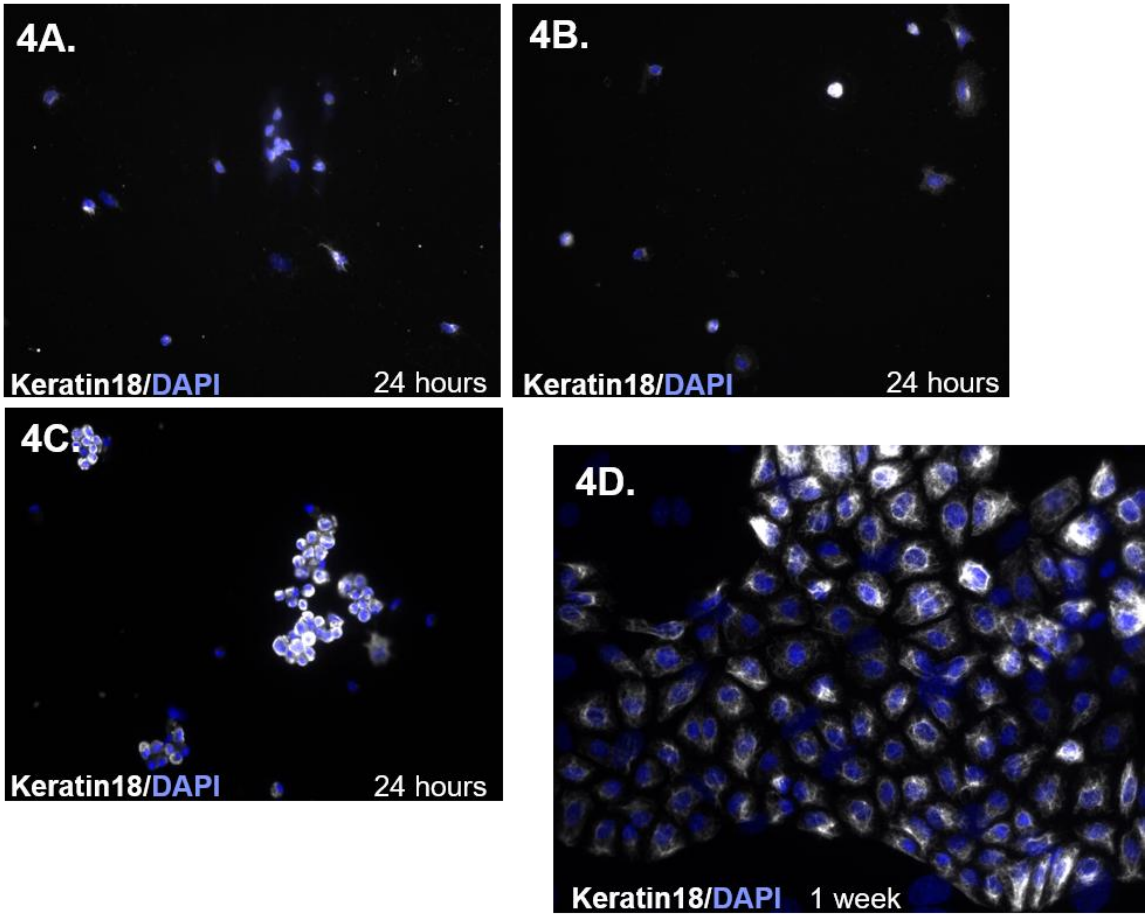

Figure 4. CD104 MACS enriches for Keratin-18^{+} cells. Cells were allowed to adhere for 24 hours before fixation. Immunofluorescent detection of Keratin-18 (300 ms exposure) and DAPI (20 ms exposure), Images captured at 40x. (A) Before sort, the heart digest technique provides a population abundant in Keratin-18+ cells. (B) Fewer Keratin-18+ cells exist in culture in the post-sort negative fraction fixed 24 hours after enzymatic digest. (C) Culture is abundant in Keratin-18+ cells after CD104 MACS. (D) One week after digest, cells from the CD104^{+} MACS population expand in culture and maintain a cobblestone-like morphology. Keratin-18^{+} intermediate filaments are still expressed.

3.3 Greater overall number of epicardial cells isolated from hearts of running mice

Mice were allowed to run *ad libitum* for 1 week prior to epicardial cell isolation. We measured the distance run each day by odometer and observed that mice primarily ran at night, with an average distance of 7.32 ± 2.90 km/day (4.55 ± 1.80 miles/day, n = 4). Of interest, we performed cell counts after CD104 MACS and observed a significant increase in total number of cells per heart for isolates from running mice (Control mice: 15,000 ± 3,100 cells/heart; Running mice: 38,300 ± 7,100 cells/heart; n=5 mice per group; 2-tailed t-test, $p < 0.01$). Spectrophotometer measurements after total RNA isolation showed that we obtained 27.4 ± 6.5 ng/μL of RNA from control mice (n = 10 total) and 74.0 ± 2.7 ng/μl of RNA from running-exercised mice (n = 10 total).

3.4 Microarray assays and bioinformatic analysis to determine epicardial cell gene expression in runners and non-runners

To examine epicardial gene expression for runners and non-runners, we pooled epicardial cells isolated by CD104 MACS from the hearts of healthy control mice and those that ran *ad libitum* for 1 week (n =5/group). Based on our unpublished observations from epicardial cell lineage-tracing studies in transgenic mice at 2 weeks after running-exercise (Rao et al., under review), we hypothesized that we could capture an active transcriptional response in running mice after 1 week of running that would differ from that of non-runners. Samples were pooled to help normalize: 1) Variation in the number of epicardial cells isolated from individual mice (e.g., low relative cell number isolated

from controls), and 2) Variation in the distance run among runners. For runners and non-runners, global gene transcription profiles were generated from fresh isolates of epicardial cells that were immediately lysed for total RNA isolation; this RNA was used to produce biotinylated cDNA probes. The cDNA probes were then hybridized to Affymetrix cDNA microarrays **(**GeneChip Mouse Gene 2.0 ST Array**).**

For bioinformatic analysis, gene expression data were averaged for 2 samples (n = 5 mice /sample), statistically-filtered (Cut-off of 2.0 for relative log expression [RLE]), and analyzed for quality control, based on the variation of the median and quartiles probe set intensities (See Appendix, Figure 6). To perform functional clustering, the filtered gene expression data were entered into the Database for Annotation, Visualization, and Integrated Discovery (DAVID) (Huang et al., 2009) and also grouped according to Gene Onology (GO) terms. This analysis identified genes with significant changes in expression and grouped them into 3 major GO domains: Biological process, Cellular process, and Molecular function. At a higher level of resolution, we examined the top GO terms identified from each of the 3 categories. These genes belonged to: “extracellular matrix” (ECM), GO:0031012; “nucleic acid binding transcription factor activity”, GO:0001071; and “reproductive”, GO:0022414 (Fig. 5). Based on our interests in angiogenesis, vascular rescue/repair, and perfusion, in addition to the 3 major GO term-associated gene sets, we also focused our attention on vascular-related gene expression.

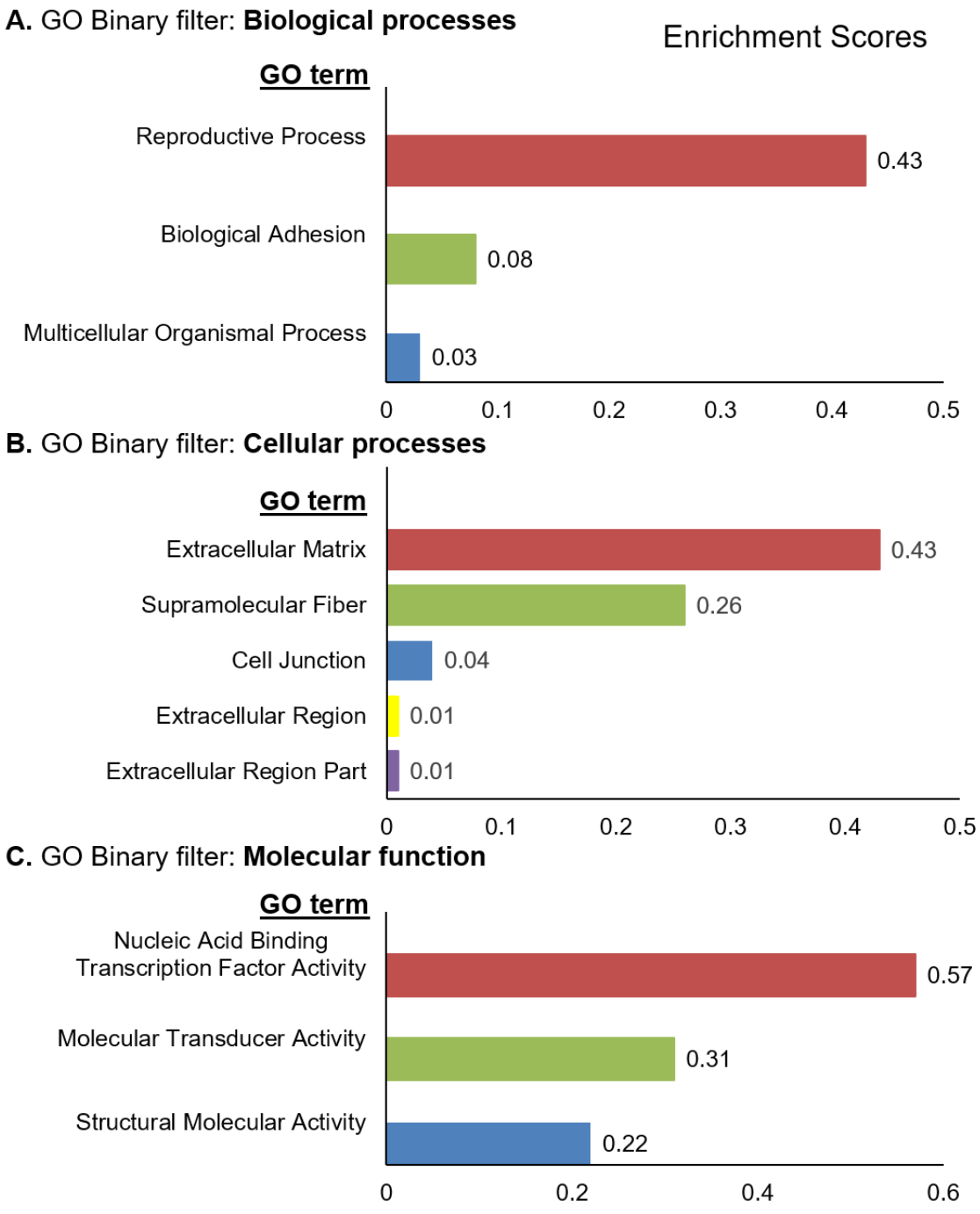

Figure 5. Functional clustering from DAVID analysis using GO domain filters. Top results from each category shown.

3.4.1 Changes in "Reproductive Process" of the GO biological process domain

Within the GO domain for biological processes, the GO term (GO:0022414), "reproductive," filtered 1250 transcripts, of which 110 significantly differed between samples ($p < 0.05$) (Table 2). Our results demonstrated a significant decrease ($p < 0.01$) in gene expression for the mitochondrial proteins Bcl2 (fold-change = -1.27) and Immpl1 (fold-change = - 1.41), as well as Prdx4, a member of the peroxiredoxin family (fold-change = -1.61). We also observed a significant increase ($p < 0.01$) in gene expression for Lrp6, a Wnt-signaling receptor (fold-change = 1.13).

Table 2. Reproductive Genes and Fold-Change in Response to Running Exercise.

Gene Symbol	Gene Description	Δ Running vs Non-running	
		Fold-change	p-value
Bcl2	Outer mitochondrial membrane protein involved in apoptotic mechanisms	-1.27	0.0003
Immp2l	Encodes a mitochondria-targeted signal peptide sequence and inner mitochondrial membrane protein	-1.41	0.001
Prdx4	Involved in the reduction of H_2O_2	-1.61	0.0005
Lrp6	Wnt co-receptor, involved in cytoplasmic β-catenin accumulation	1.13	0.002

3.4.2 Changes in the "Extracellular Matrix" of the cellular process GO domain

We found that 386 gene transcripts clustered with the GO term for ECM (GO:0031012). Running induced a significant change for 36 ECM-associated genes in isolated $CD104^{+}$ epicardial cells ($p < 0.05$) (Table 3); these included genes with upregulated expression: glypican 5 (Gpc5), ladinin (Lad1), collagen, type VII, alpha 1 (Col7a1); and those that were down-regulated: vitrin (Vit), collagen, type VI, alpha 1 (Col6a1). We selected these transcripts based on our interest in extracellular matrix remodeling and/or involvement in cell migration.

Table 3. ECM-related Genes and Fold-Change in Response to Running Exercise.

Gene Symbol	Gene Description	Δ Running vs Non-running	
		Fold-change	p-value
Gpc5	Plasma membrane bound heparin sulfate proteoglycan	1.49	0.035
Lad1	Anchoring filament	1.35	0.022
Col7a1	ECM component	1.32	0.019
Vit	Matrix assembly, GAG binding	-1.73	0.018
Col6a1	ECM component	-1.30	0.040

3.4.3 Changes in vascular-related genes and in "Nucleic Acid Transcription Factor Binding" genes from the Molecular Function GO domain

We found that 1088 genes clustered with the GO term "nucleic acid transcription factor binding" (GO:0001071). Eighty-two of these differed significantly between the samples from runners and non-runners ($p < 0.05$). Within the Forkhead box (FOX) family of transcription factors, mRNAs for FoxA3, FoxG1, and FoxS1 were significantly upregulated ($p < 0.05$) (Table 4). Of note, gene expression for TCF21, an important transcription factor for fibroblast specification, was down-regulated in isolated epicardial cells of runners compared with non-runners (Table 4).

Regarding the ability of epicardial cells to contribute to neovascularization, our microarray analysis indicated a significant ($p < 0.05$) increase in gene transcription for vascular endothelial growth factor B (Vegfb; fold change = 1.36), endothelin-3 (Edn3; fold change = 1.23), and angiogenin-6 (Ang6; fold change = 1.35) (Table 5).

Table 4. Transcription factor-related Genes and Fold-Change in Response to Running Exercise.

Gene Symbol	Gene Description	Δ Running vs Non-running	
		Fold-change	p-value
FoxA3	Regulates hematopoetic stem and progenitor cell survival	1.37	0.02
FoxG1	Cell differentiation	1.53	0.00008
FoxS1	Development and differentiation	-1.37	0.037
TFC21	Fibroblast-specific transcription regulator	-1.42	0.09

Table 5. Vasculature-related Genes and Fold-Change in Response to Running Exercise.

Gene Symbol	Gene Description	Δ Running vs Non-running	
		Fold-change	p-value
Vegfb	Flt-1 ligand, involved in angiogenesis and vascular development	1.36	0.07
Edn3	Vasoactive protein, stimulates endothelial cell migration in culture	1.23	0.006
Ang6	Angiogenic ribonuclease	1.35	0.047

3.4.4 Running-exercise significantly changes transcript expression compared with control mice.

Of the 41,345 transcripts identified by microarray, expression of Snord116 increased the most in running-exercised mice (fold-change = 7.08, p-value = 0.044) and Igk-V28 decreased the most in running-exercised mice (fold-change = -3.84, p = 0.037). We list the transcripts with the largest fold-change that were significantly different between running-exercised and control mice in Table 6.

Table 6. Gene expression data for the most prominent fold-changes from running-exercised ("Running") mice. Left, increases in transcript fold-change and Right, decrease in transcript fold change, relative to the running-exercised sample.

Up in Running			Down in Running		
Gene name	**Fold-change**	**p-value**	**Gene name**	**Fold-change**	**p-value**
Snord116	7.08	0.044	Igk-V28	-3.84	0.037
Mir101c	6.17	0.020	Zfp125	-3.13	0.008
Gm9602	4.91	0.034	Xlr3b	-3.12	0.044
Srsy	4.74	0.010	Gm13034	-3.04	0.031
Ssty2	4.22	0.041	Mirlet7f-1	-3.02	0.026
MGC107098	3.70	0.038	Snord61	-2.94	0.023
Gm2046	3.46	0.015	Omd	-2.64	0.008
Ssty1	3.05	0.001	Zfp932	-2.60	0.049
Sly	3.12	0.047	Pyhin1	-2.47	0.036

Chapter 4: DISCUSSION

4.1 Advantages and limitations of our method for isolation of primary murine epicardial cells

To isolate primary epicardial cells directly from the adult mouse heart, we developed a protocol that minimized exposure to cell culture plastic and medium. We used collagenase/dispase to digest ECM components (Gibson et al. 1989; Hu et al. 2006; Oseni et al. 2013), since trypsin can potentially destroy cell surface epitopes (such as CD104) and other proteins (Shoelson et al. 1988; Nakayama et al. 2004; Huang et al. 2010). Although some commercially available products require less than 1 hour for cell isolation, they yield a highly heterogeneous cell population because they completely dissociate cardiac tissue (e.g. MACS Tissue Dissociation Kits, Miltenyi Biotech). Our method required 2 hours, but primarily isolated epicardial cells directly from the heart cover. Furthermore, to increase cell survival, we used the mitochondrial transition pore inhibitor cyclosporine A (CsA, 10 μM) (Zamzami et al. 1996; Jung et al. 2008; Sachewsky et al. 2014). Although this concentration of CsA increased cell viability, in the future we will generate survival curves to identify an optimal CsA concentration.

Differing from currently published isolation methods for adult epicardial cells and EPDC, our protocol employed CD104 MACS. In the future, further enrichment by FACS may be possible with a second primary antibody specific to a different cell surface protein on epicardial cells. To further purify native epicardial cells, we could also try to

remove contaminating blood cells with antibodies to CD45 (CD45 MACS). In this case, the CD45-negative fraction would then be used for CD104 MACS.

4.2 Transcriptional profiling of undifferentiated CD104+epicardial cells isolated from the hearts of running-exercised and non-running mice

Based on the role(s) that epicardial cells play in blood vessel formation during cardiac development and vascular repair after injury (Smart et al. 2007; Smart et al. 2010), we hypothesized that undifferentiated ($CD104^{+}/K18^{+}$) epicardial cells contribute to angiogenesis and/or vascular remodeling during cardiac hypertrophy due to running exercise. In order to address this experimentally, we developed a protocol for primary epicardial cell isolation directly from the cover of the adult murine heart and used it to compare global gene expression profiles of epicardial cells isolated from the hearts of mice that engaged in running-exercise for 1 week to those of healthy, non-running mice that served as controls. Because epicardial cells may undergo EMT during running exercise to directly form microvascular endothelial cells, or engage in paracrine activity that supports angiogenesis, understanding changes in gene transcription that occur in native epicardial cells from the heart surface may provide insight into key molecules or signaling pathways that can be targeted to provide benefit to patients with cardiac injury.

For our running-exercise paradigm, mice were housed either with or without a running wheel for 1 week before heart digest and epicardial cell isolation. We chose the 1-week time point in order to capture early transcriptional changes of the epicardium in

running-exercised mice. To address potential variability between mice in the same group (running or non-running), we pooled samples from each condition (n =5 mice per group). Notably, while this approach provides a reasonable overall picture of gene activity within a group (i.e., runners or non-runners), it does not allow us to correlate actual running distance for mouse "A" with specific transcript changes in mouse "A". For future studies, attaining this level of resolution may be possible with further improvements in cell isolation to obtain greater amounts of material, RNA isolation efficiency, and gene profiling technology.

To identify primary epicardial cells, we performed immunocytochemistry for Keratin 18, an epithelial intermediate filament protein expressed by epicardial cells on the cover of the heart, but not by other cardiac cell-types. After cell isolation, we consistently obtained a greater number of epicardial cells ($K18^{+}$) from heart digests of running-exercised mice compared with non-runners. Importantly, we found this to be the case both before and after CD104 MACS, indicating that the difference may relate to the condition of the heart prior to tissue digestion/cell isolation. For example, the composition of ECM components could be altered during remodeling in response to running. Of interest, our microarray analysis supports this hypothesis as demonstrated by: 1) Functional clusters from DAVID analysis, 2) GO term enrichment scores for ECM, and 3) Expression data for particular ECM-related genes. Altogether, our data for ECM-related gene expression in epicardial cells from runners and non-runners suggest a pattern of ECM degradation and remodeling in runners; this may explain the observed increase in overall number of epicardial cells obtained after heart digestion with

collagenase/dispase. Accordingly, the overall amount of collagen or compliment of collagen species present in the epicardial basement membrane may differ between runners and non-runners. To address this question, we have repeated our running study and isolated $CD104^{+}$ epicardial cells from the hearts of individual mice (Non-runners, 21,778 ± 6,500 cells per heart; Runners, 39,533 ± 1,750 cells per heart; N=5 hearts per condition). Using these cells, further studies may examine candidate ECM proteins or ECM-related proteins by Western blot or ELISA to verify the preliminary microarray screen (some candidates are listed below in 4.2).

4.3 Running-exercise modifies the expression of gene transcripts listed under the "Reproductive" GO term

Running exercise may affect mitochondrial function in epicardial cells (or, a subpopulation thereof) to promote an "activated state" before subsequent migration through the subepicardial extracellular matrix (Kocabas et al. 2012). In our analysis, we identified a significant decrease ($p < 0.01$) in the inner mitochondria membrane peptidase Immp2l (fold change = -1.41) and the outer mitochondrial membrane protein Bcl2 (fold change = -1.27). Lu *et al.* (2008) show an increase in ATP production in isolated mitochondria from Immp2l deficient mice, which might be advantageous for activated epicardial cells (Lu et al. 2008). The role of the pro-survival protein, Bcl2, is tissue-specific and context dependent (Reviewed in Sochalska et al. 2015). In future experiments, it would be interesting to measure metabolic changes such as oxygen consumption, ATP production, and/or glycolytic flux to determine whether there are

differences in bioenergetics between running-exercised epicardial cells and those of non-runners.

We observed a subtle, yet significant increase in expression in epicardial cells from exercised mice of low-density lipoprotein receptor-related protein 6 (Lrp6; fold change = 1.13, $p < 0.05$). In our lab, we identified Lrp6 as an epicardial cell surface receptor for CTGF-D4 that mediates EPDC graft success by increasing Sox9 levels, which regulates Endothelin Receptor B expression; this receptor is required for EPDC proliferation and migration after MI (Rao et al., PhD dissertation; University of Vermont).

4.4 Epicardial gene expression suggests extracellular matrix remodeling in the running heart

Many genes that grouped with the GO term ECM such as MMP10 and ADAM family members indicate that running may induce ECM degradation or modification (Appendix 1). Running-induced cardiac hypertrophy may require remodeling of extracellular matrix proteins that form the epicardial basement membrane. For example, strain on the heart or increase in heart size may elicit changes in relative concentration or composition of different collagen isoforms. Col7a1 contributes to matrix adhesion by anchoring collagen fibrils to adhesion molecules; its expression significantly decreases in epicardial cells lacking PDGFR, which contributes to epicardial EMT failure (Sakai et al. 1986; Chung & Uitto 2010; Smith et al. 2011). In our data set, gene expression for other collagen isoforms, such as Col6a1, was significantly down-regulated (fold change = -

1.30, $p < 0.05$). In 2012, Luther *et al.* (2012) demonstrated that after permanent occlusion of the left anterior descending artery, mice deficient in Col6a1 ($Col6a1^{-/-}$) had decreased collagen deposition after surgery and an unexpected improvement in cardiac function as assessed by echocardiography (Luther et al. 2012). These results suggest that the absence of Col6a may benefit cardiac function and remodeling after infarction.

We observed significant increases ($p < 0.05$) in gene expression for both structural and signaling ECM components including the anchoring protein Lad1 (a.k.a. Col17A1 ectodomain, fold change = 1.35) and GPI-anchored glypican, GPC5 (fold-change = 1.49), which is likely involved in growth factor signal transduction (Moll & Moll 1998; Franzke et al. 2002; Walko et al. 2015; Ibrahimi et al. 2004; Williamson et al. 2007; Li et al. 2011; Filmus & Capurro 2014). In cancer, Lad1 down-regulation during metastatic EMT contributes to overall ECM re-arrangement (Thomson et al. 2011; Gröger et al. 2012). Based on this observation, we predict that Lad1 upregulation supports the increase in epicardial cell density in running-exercised mice. To better understand the role of GPC5, we could use immunocytochemistry to determine its cellular localization/distribution.

Of interest, running may also require various components of the subepicardial extracellular matrix to be degraded to allow for EPDC migration after epicardial EMT (Combs et al. 2011; Tao et al. 2013). We observed a decrease (fold change = -1.73) in the matrix-assembly protein Vitrin (Whittaker & Hynes 2002).

4.5 Running induces vasculature-related signaling in epicardial cells

Cardiomyocytes require neovascularization to support exercised-induced ventricular hypertrophy and we expected running-exercise to induce cardiac angiogenesis. By microarray assays, although the transcript for VEGF-A did not change, the transcript for VEGFB increased by 1.36-fold ($p = 0.07$) in runners compared with non-runners. VEGFB is a selective ligand for Flt-1 (VEGFR-1) and VEGFB signaling that supports vascular development in the heart and angiogenesis (Olofsson et al. 1996; Cross et al. 2003; Lähteenvuo et al. 2009; Jensen et al. 2015). After ischemic injury, VEGFB is reported to act as a blood vessel survival factor, rather than a proliferation or growth factor (Bellomo et al. 2000; Wright 2002; Zhang et al. 2009)

Avian EPDC were shown to contribute endothelial cells during development and the authors suggested that VEGF or PDGF signaling may be involved (Pérez-Pomares et al. 2002; Guadix et al. 2006). At present, it is controversial whether adult EPDC in mammals are shifted toward an endothelial cell fate after MI. In mice, Zamora *et al.* (2007) found that an epicardial β-catenin was required for coronary artery formation. Although their data did not demonstrate direct differentiation from epicardial cells to endothelial cells per se, their results do suggest a requirement for EPDC signaling in vascular development (Zamora et al. 2007). Overexpression of prokineticin receptor-1 in cardiomyocytes promotes EPDC differentiation to endothelial cells in explant culture; this suggests that EPDC-derived endothelial cells may participate in neovascularization (Urayama et al. 2008).

We observed an increase in Edn3 transcript expression (fold-change = 1.23, $p < 0.01$) in response to running exercise. Both hypoxic conditions and the vasoactive

protein endothelin-3 (EDN3) can stimulate VEGF production, as detected by both luciferase/VEGF promoter reporter activity and anti-VEGF antibody (Rao et al. 1991; Levy et al. 1995; Pedram et al. 1997). EDN3 was shown to stimulate endothelial cell migration in culture (Morbidelli et al. 1995).

In running-exercised mice, the gene transcript for Ang6 significantly increased (fold change = 1.35, $p < 0.05$). A known angiogenic ribonuclease, soluble angiogenin binds endothelial cell surface receptors, is endocytosed, and then is trafficked to the nucleus where it participates in ribosomal RNA transcription (Moroianu & Riordan 1994; Adams & Subramanian 1999; Xu et al. 2002). Endocytosis and nuclear trafficking of angiogenin is critical to [calf pulmonary artery] endothelial cell proliferation (Moroianu & Riordan 1994). Kishimoto *et al.* (2005) demonstrated that the nuclear translocation of angiogenin is required for VEGF-stimulated angiogenesis (Kishimoto et al. 2005).

4.6 FOX and ETS transcription factors expression increases in epicardial cells after running exercise

In our microarray analysis, we identified the upregulation of members of the FOX family of transcription factors that are involved in cellular differentiation and vascular development. For example, FoxG1 is critical for differentiation of thymic epithelial cells, neural cells, and embryonic stem cells (Wei & Condie 2011; Yamamizu et al. 2013; Pancrazi et al. 2015). FoxA3 regulates hematopoetic stem and progenitor cell survival and, in combination with tumor necrosis factor receptor 1, promotes liver regeneration (Holmfeldt et al. 2016; Wangensteen et al. 2015). Using a FoxS1 knock-in reporter

mouse, Heglind *et al.* (2005) demonstrated FoxS1 expression in vascular smooth muscle cells and pericytes on the brain surface (Heglind et al. 2005). FoxS1 is also expressed in pericytes and Sertoli cells of fetal testis and is required for the development of testicular vasculature, as shown in FoxS1 deficient mice (Sato et al. 2008). FoxS1 is part of a major regulatory network that promotes fibroblast to myofibroblast differentiation (Noizet et al. 2015). In epicardial cells, it is likely that a combination of FOX and ETS transcription factors regulate both cell differentiation and endothelial gene expression via the FOX: ETS motif (Dejana et al. 2007; De Val et al. 2008).

4.7 Changes in epicardial gene expression: implications for human health and disease

Our microarray data have potential to impact human health and disease treatment. Among all transcripts, Snord116 (HBII-85) was upregulated the most in epicardial cells from running mice (~7-fold, $p > 0.05$). The Snord116 locus contains multiple snoRNAs and is best known for its role in alternative splicing of the serotonin receptor gene in mammals (Schüle et al. 2005; Skryabin et al. 2007). Among non-coding RNAs, C/D box small nucleolar RNAs (snoRNA) help direct rRNA modifications (2'-*O*-ribose methylation) and facilitate pre-mRNA splicing (Kiss 2002; Yin et al. 2012). Importantly, the Snord116 locus controls the expression of approximately 200 genes (coding regions). As such, snoRNAs from the Snord116 locus may regulate some of the metabolic changes that occur in response to running exercise.

Translocation or deletion of the Snord116 locus was shown to contribute to a rare neurodevelopmental disorder called Prader-Willis Syndrome (PWS) (Bieth et al. 2015; Zieba et al. 2015). Mouse models of PWS have been developed that share several phenotypic characteristics with patients (Ding et al. 2008). Snord116-deficient mice ($Snord116^{-/-}$) were shown to both eat more and expend more energy than did control mice ($Snord116^{+/+}$) (Qi et al. 2016). For our work, it is clearly of interest to determine whether changes in epicardial cells contribute to the altered metabolism of $Snord116^{-/-}$ mice. Also, compared with wildtype mice, would $Snord116^{-/-}$ mice be physically capable of running for similar distance and duration? Does exercise promote ventricular hypertrophy in Snord116-deficient mice? If so, will the observed changes in gene expression for extracellular matrix proteins, vascular signaling proteins, and transcription factors that occur in the epicardial cells of wildtype running mice be maintained in running Snord116 deficient mice? Such investigations could provide interesting insights into PWS manifestation as well as rationale for drug development.

This analysis was originally designed to screen for epicardial-specific factors that promote cardiovascular perfusion by either direct differentiation (endothelial lineage specification) or through indirect paracrine signaling mechanisms (angiogenesis). For direct differentiation, it may be possible to prime epicardial cells *ex vivo* for endothelial specification prior to delivery by tangential injection into the subepicardium after MI. Our research group has shown that subepicardial injection can markedly improve graft success after MI (Iso, et al. 2014). In terms of paracrine activity, specific factors identified in running-exercised mice may either protect existing blood vessels or stimulate new vessel growth. To this end, our microarray analysis could serve as a valuable screen for epicardial-derived factors with potential to act as powerful angiogenic therapeutics either alone or in combination.

References

Adams, S.A. & Subramanian, V., 1999. The angiogenins: an emerging family of ribonuclease related proteins with diverse cellular functions. *Angiogenesis*, 3(3), pp.189–99.

Asahara, T. et al., 1999. VEGF contributes to postnatal neovascularization by mobilizing bone marrow-derived endothelial progenitor cells. *The EMBO journal*, 18(14), pp.3964–72.

Bellomo, D. et al., 2000. Mice lacking the vascular endothelial growth factor-B gene (Vegfb) have smaller hearts, dysfunctional coronary vasculature, and impaired recovery from cardiac ischemia. *Circulation research*, 86(2), pp.E29–35. Available at:

Benjamini, Y, and Y Hochberg. 1995. Controlling the false discovery rate: a practical and powerful approach to multiple testing. JRSS, B, 57, 289-300.

Bieth, E. et al., 2015. Highly restricted deletion of the SNORD116 region is implicated in Prader-Willi Syndrome. *European journal of human genetics : EJHG*, 23(2), pp.252–5.

Cano, A. et al., 2000. The transcription factor snail controls epithelial-mesenchymal transitions by repressing E-cadherin expression. *Nature cell biology*, 2(2), pp.76–83.

Chung, H.J. & Uitto, J., 2010. Type VII collagen: the anchoring fibril protein at fault in dystrophic epidermolysis bullosa. *Dermatologic clinics*, 28(1), pp.93–105.

Cochain, C., Channon, K.M. & Silvestre, J.-S., 2013. Angiogenesis in the infarcted myocardium. *Antioxidants & redox signaling*, 18(9), pp.1100–13.

Combs, M.D. et al., 2011. NFATC1 promotes epicardium-derived cell invasion into myocardium. *Development (Cambridge, England)*, 138(9), pp.1747–57.

Cross, M.J. et al., 2003. VEGF-receptor signal transduction. *Trends in biochemical sciences*, 28(9), pp.488–94.

Dejana, E., Taddei, A. & Randi, A.M., 2007. Foxs and Ets in the transcriptional regulation of endothelial cell differentiation and angiogenesis. *Biochimica et biophysica acta*, 1775(2), pp.298–312.

Dettman, R.W. et al., 1998. Common epicardial origin of coronary vascular smooth muscle, perivascular fibroblasts, and intermyocardial fibroblasts in the avian heart. *Developmental biology*, 193(2), pp.169–81.

Ding, F. et al., 2008. SnoRNA Snord116 (Pwcr1/MBII-85) deletion causes growth deficiency and hyperphagia in mice. *PloS one*, 3(3), p.e1709.

Dirkx, E., da Costa Martins, P.A. & De Windt, L.J., 2013. Regulation of fetal gene expression in heart failure. *Biochimica et biophysica acta*, 1832(12), pp.2414–24.

Evans, S.M. et al., 2010. Myocardial lineage development. *Circulation research*, 107(12), pp.1428–44.

Felician, G. et al., 2014. Epigenetic modification at Notch responsive promoters blunts efficacy of inducing notch pathway reactivation after myocardial infarction. *Circulation research*, 115(7), pp.636–49.

Filmus, J. & Capurro, M., 2014. The role of glypicans in Hedgehog signaling. *Matrix biology : journal of the International Society for Matrix Biology*, 35, pp.248–52.

Franzke, C.-W. et al., 2002. Transmembrane collagen XVII, an epithelial adhesion protein, is shed from the cell surface by ADAMs. *The EMBO journal*, 21(19), pp.5026–35.

Gibson, P.R. et al., 1989. Isolation of colonic crypts that maintain structural and metabolic viability in vitro. *Gastroenterology*, 96(2 Pt 1), pp.283–91.

Von Gise, A. & Pu, W.T., 2012. Endocardial and epicardial epithelial to mesenchymal transitions in heart development and disease. *Circulation research*, 110(12), pp.1628–45.

Greulich, F. et al., 2012. Tbx18 function in epicardial development. *Cardiovascular research*, 96(3), pp.476–83.

Gröger, C.J. et al., 2012. Meta-analysis of gene expression signatures defining the epithelial to mesenchymal transition during cancer progression. *PloS one*, 7(12), p.e51136.

Guadix, J.A. et al., 2006. In vivo and in vitro analysis of the vasculogenic potential of avian proepicardial and epicardial cells. *Developmental dynamics : an official publication of the American Association of Anatomists*, 235(4), pp.1014–26.

Heglind, M. et al., 2005. Lack of the central nervous system- and neural crest-expressed forkhead gene Foxs1 affects motor function and body weight. *Molecular and cellular biology*, 25(13), pp.5616–25.

Holmfeldt, P. et al., 2016. Functional screen identifies regulators of murine hematopoietic stem cell repopulation. *The Journal of experimental medicine*, 213(3), pp.433–49.

Horckmans, M. et al., 2016. Neutrophils orchestrate post-myocardial infarction healing by polarizing macrophages towards a reparative phenotype. *European heart journal*, p.ehw002–.

Hu, X., Jiang, Z. & Liu, N., 2006. A novel approach for harvesting lymphatic endothelial cells from human foreskin dermis. *Lymphatic research and biology*, 4(4), pp.191–8.

Huang, D.W., Sherman, B.T. & Lempicki, R.A., 2009. Systematic and integrative analysis of large gene lists using DAVID bioinformatics resources. *Nature protocols*, 4(1), pp.44–57.

Huang, H.-L. et al., 2010. Trypsin-induced proteome alteration during cell subculture in mammalian cells. *Journal of biomedical science*, 17(1), p.36.

Ibrahimi, O.A. et al., 2004. Kinetic model for FGF, FGFR, and proteoglycan signal transduction complex assembly. *Biochemistry*, 43(16), pp.4724–30.

Iso, Y. et al., 2014. Priming with ligands secreted by human stromal progenitor cells promotes grafts of cardiac stem/progenitor cells after myocardial infarction. *Stem cells (Dayton, Ohio)*, 32(3), pp.674–83.

Jensen, L.D. et al., 2015. VEGF-B-Neuropilin-1 signaling is spatiotemporally indispensable for vascular and neuronal development in zebrafish. *Proceedings of the National Academy of Sciences of the United States of America*, 112(44), pp.E5944–53.

Jung, J.-Y. et al., 2008. Inhibition of apoptotic signals in overgrowth of human gingival fibroblasts by cyclosporin A treatment. *Archives of oral biology*, 53(11), pp.1042–9.

Kehat, I. & Molkentin, J.D., 2010. Molecular pathways underlying cardiac remodeling during pathophysiological stimulation. *Circulation*, 122(25), pp.2727–35. Available at:

Kim, J. et al., 2012. In vitro culture of epicardial cells from adult zebrafish heart on a fibrin matrix. *Nature protocols*, 7(2), pp.247–55.

Kishimoto, K. et al., 2005. Endogenous angiogenin in endothelial cells is a general requirement for cell proliferation and angiogenesis. *Oncogene*, 24(3), pp.445–56.

Kiss, T., 2002. Small Nucleolar RNAs. *Cell*, 109(2), pp.145–148.

Kocabas, F. et al., 2012. The hypoxic epicardial and subepicardial microenvironment. *Journal of cardiovascular translational research*, 5(5), pp.654–65.

Lähteenvuo, J.E. et al., 2009. Vascular endothelial growth factor-B induces myocardium-specific angiogenesis and arteriogenesis via vascular endothelial growth factor receptor-1- and neuropilin receptor-1-dependent mechanisms. *Circulation*, 119(6), pp.845–56.

Lamouille, S., Xu, J. & Derynck, R., 2014. Molecular mechanisms of epithelial-mesenchymal transition. *Nature reviews. Molecular cell biology*, 15(3), pp.178–96.

Levy, A.P. et al., 1995. Transcriptional Regulation of the Rat Vascular Endothelial Growth Factor Gene by Hypoxia. *Journal of Biological Chemistry*, 270(22), pp.13333–13340.

Li, F. et al., 2011. Glypican-5 stimulates rhabdomyosarcoma cell proliferation by activating Hedgehog signaling. *The Journal of cell biology*, 192(4), pp.691–704.

Lu, B. et al., 2008. A mutation in the inner mitochondrial membrane peptidase 2-like gene (Immp2l) affects mitochondrial function and impairs fertility in mice. *Biology of reproduction*, 78(4), pp.601–10.

Luther, D.J. et al., 2012. Absence of type VI collagen paradoxically improves cardiac function, structure, and remodeling after myocardial infarction. *Circulation research*, 110(6), pp.851–6.

Männer, J. et al., 2001. The origin, formation and developmental significance of the epicardium: a review. *Cells, tissues, organs*, 169(2), pp.89–103.

Masters, M. & Riley, P.R., 2014. The epicardium signals the way towards heart regeneration. *Stem cell research*, 13(3 Pt B), pp.683–92.

Moll, R. & Moll, I., 1998. Epidermal adhesion molecules and basement membrane components as target structures of autoimmunity. *Virchows Archiv : an international journal of pathology*, 432(6), pp.487–504.

Morbidelli, L. et al., 1995. Proliferation and migration of endothelial cells is promoted by endothelins via activation of ETB receptors. *The American journal of physiology*, 269(2 Pt 2), pp.H686–95.

Moroianu, J. & Riordan, J.F., 1994. Nuclear translocation of angiogenin in proliferating endothelial cells is essential to its angiogenic activity. *Proceedings of the National Academy of Sciences of the United States of America*, 91(5), pp.1677–81.

Mozaffarian, D. et al., 2016. Executive Summary: Heart Disease and Stroke Statistics-2016 Update: A Report From the American Heart Association. *Circulation*, 133(4), pp.447–54.

Murphy, E. & Steenbergen, C., 2008. Mechanisms underlying acute protection from cardiac ischemia-reperfusion injury. *Physiological reviews*, 88(2), pp.581–609.

Nakayama, T. et al., 2004. Inactivation of protease-activated receptor-1 by proteolytic removal of the ligand region in vascular endothelial cells. *Biochemical pharmacology*, 68(1), pp.23–32.

Nandi, S.S. & Mishra, P.K., 2015. Harnessing fetal and adult genetic reprograming for therapy of heart disease. *Journal of nature and science*, 1(4).

Noizet, M. et al., 2015. Master regulators in primary skin fibroblast fate reprogramming in a human ex-vivo model of chronic wounds. *Wound repair and regeneration : official publication of the Wound Healing Society [and] the European Tissue Repair Society*.

Olofsson, B. et al., 1996. Vascular endothelial growth factor B, a novel growth factor for endothelial cells. *Proceedings of the National Academy of Sciences of the United States of America*, 93(6), pp.2576–81.

Olson, E.N., 2006. Gene regulatory networks in the evolution and development of the heart. *Science (New York, N.Y.)*, 313(5795), pp.1922–7.

Oseni, A.O., Butler, P.E. & Seifalian, A.M., 2013. Optimization of chondrocyte isolation and characterization for large-scale cartilage tissue engineering. *The Journal of surgical research*, 181(1), pp.41–8.

Pancrazi, L. et al., 2015. Foxg1 localizes to mitochondria and coordinates cell differentiation and bioenergetics. *Proceedings of the National Academy of Sciences of the United States of America*, 112(45), pp.13910–5.

Pasotti, M., Prati, F. & Arbustini, E., 2006. The pathology of myocardial infarction in the pre- and post-interventional era. *Heart (British Cardiac Society)*, 92(11), pp.1552–6.

Pedram, A. et al., 1997. Vasoactive Peptides Modulate Vascular Endothelial Cell Growth Factor Production and Endothelial Cell Proliferation and Invasion. *Journal of Biological Chemistry*, 272(27), pp.17097–17103.

Pérez-Pomares, J.-M. et al., 2002. Origin of coronary endothelial cells from epicardial mesothelium in avian embryos. *The International journal of developmental biology*, 46(8), pp.1005–13.

Pérez-Pomares, J.M. & Muñoz-Chápuli, R., 2002. Epithelial-mesenchymal transitions: a mesodermal cell strategy for evolutive innovation in Metazoans. *The Anatomical record*, 268(3), pp.343–51.

Rao, V. V, Löffler, C. & Hansmann, I., 1991. The gene for the novel vasoactive peptide endothelin 3 (EDN3) is localized to human chromosome 20q13.2-qter. *Genomics*, 10(3), pp.840–1.

Reese, D.E., Mikawa, T. & Bader, D.M., 2002. Development of the coronary vessel system. *Circulation research*, 91(9), pp.761–8.

Sachewsky, N. et al., 2014. Cyclosporin A enhances neural precursor cell survival in mice through a calcineurin-independent pathway. *Disease models & mechanisms*, 7(8), pp.953–61.

Sakai, L.Y. et al., 1986. Type VII collagen is a major structural component of anchoring fibrils. *The Journal of cell biology*, 103(4), pp.1577–86.

Sato, Y. et al., 2008. Importance of forkhead transcription factor Fkhl18 for development of testicular vasculature. *Molecular reproduction and development*, 75(9), pp.1361–71.

Schüle, B. et al., 2005. Molecular breakpoint cloning and gene expression studies of a novel translocation t(4;15)(q27;q11.2) associated with Prader-Willi syndrome. *BMC medical genetics*, 6, p.18.

Shinde, A. V & Frangogiannis, N.G., 2014. Fibroblasts in myocardial infarction: a role in inflammation and repair. *Journal of molecular and cellular cardiology*, 70, pp.74–82..

Shoelson, S.E., White, M.F. & Kahn, C.R., 1988. Tryptic activation of the insulin receptor. Proteolytic truncation of the alpha-subunit releases the beta-subunit from inhibitory control. *The Journal of biological chemistry*, 263(10), pp.4852–60.

Skryabin, B. V et al., 2007. Deletion of the MBII-85 snoRNA gene cluster in mice results in postnatal growth retardation. *PLoS genetics*, 3(12), p.e235.

Smart, N. et al., 2010. Thymosin beta4 facilitates epicardial neovascularization of the injured adult heart. *Annals of the New York Academy of Sciences*, 1194, pp.97–104.

Smart, N. et al., 2007. Thymosin beta4 induces adult epicardial progenitor mobilization and neovascularization. *Nature*, 445(7124), pp.177–82.

Smart, N., Dubé, K.N. & Riley, P.R., 2013. Epicardial progenitor cells in cardiac regeneration and neovascularisation. *Vascular pharmacology*, 58(3), pp.164–73.

Smith, C.L. et al., 2011. Epicardial-derived cell epithelial-to-mesenchymal transition and fate specification require PDGF receptor signaling. *Circulation research*, 108(12), pp.e15–26.

Sochalska, M. et al., 2015. Lessons from gain- and loss-of-function models of pro-survival Bcl2 family proteins: implications for targeted therapy. *The FEBS journal*, 282(5), pp.834–49.

Später, D. et al., 2014. How to make a cardiomyocyte. *Development (Cambridge, England)*, 141(23), pp.4418–31.

Tao, J. et al., 2013. Epicardial HIF signaling regulates vascular precursor cell invasion into the myocardium. *Developmental biology*, 376(2), pp.136–49.

Thiery, J.P. et al., 2009. Epithelial-mesenchymal transitions in development and disease. *Cell*, 139(5), pp.871–90.

Thomson, S. et al., 2011. A systems view of epithelial-mesenchymal transition signaling states. *Clinical & experimental metastasis*, 28(2), pp.137–55.

Thorey, I.S. et al., 1993. Embryonic expression of human keratin 18 and K18-beta-galactosidase fusion genes in transgenic mice. *Developmental biology*, 160(2), pp.519–34.

Urayama, K. et al., 2008. Prokineticin receptor-1 induces neovascularization and epicardial-derived progenitor cell differentiation. *Arteriosclerosis, thrombosis, and vascular biology*, 28(5), pp.841–9.

De Val, S. et al., 2008. Combinatorial regulation of endothelial gene expression by ets and forkhead transcription factors. *Cell*, 135(6), pp.1053–64.

Walko, G., Castañón, M.J. & Wiche, G., 2015. Molecular architecture and function of the hemidesmosome. *Cell and tissue research*, 360(3), pp.529–44.

Wangensteen, K.J. et al., 2015. A genetic screen reveals Foxa3 and TNFR1 as key regulators of liver repopulation.

Wei, Q. & Condie, B.G., 2011. A focused in situ hybridization screen identifies candidate transcriptional regulators of thymic epithelial cell development and function. *PloS one*, 6(11), p.e26795.

Wessels, A. & Pérez-Pomares, J.M., 2004. The epicardium and epicardially derived cells (EPDCs) as cardiac stem cells. *The anatomical record. Part A, Discoveries in molecular, cellular, and evolutionary biology*, 276(1), pp.43–57.

White, H.D. et al., 2014. Clinical implications of the Third Universal Definition of Myocardial Infarction. *Heart (British Cardiac Society)*, 100(5), pp.424–32.

Van Wijk, B. et al., 2012. Cardiac regeneration from activated epicardium. *PloS one*, 7(9), p.e44692.

Williamson, D. et al., 2007. Role for amplification and expression of glypican-5 in rhabdomyosarcoma. *Cancer research*, 67(1), pp.57–65.

Wright, C.E., 2002. Effects of vascular endothelial growth factor (VEGF)A and VEGFB gene transfer on vascular reserve in a conscious rabbit hindlimb ischaemia model. *Clinical and experimental pharmacology & physiology*, 29(11), pp.1035–9.,

Xin, M., Olson, E.N. & Bassel-Duby, R., 2013. Mending broken hearts: cardiac development as a basis for adult heart regeneration and repair. *Nature reviews. Molecular cell biology*, 14(8), pp.529–41.

Xu, Z. et al., 2002. The nuclear function of angiogenin in endothelial cells is related to rRNA production. *Biochemical and biophysical research communications*, 294(2), pp.287–92.

Yamamizu, K. et al., 2013. Identification of transcription factors for lineage-specific ESC differentiation. *Stem cell reports*, 1(6), pp.545–59.

Yin, Q.-F. et al., 2012. Long noncoding RNAs with snoRNA ends. *Molecular cell*, 48(2), pp.219–30.

Zamora, M., Männer, J. & Ruiz-Lozano, P., 2007. Epicardium-derived progenitor cells require beta-catenin for coronary artery formation. *Proceedings of the National Academy of Sciences of the United States of America*, 104(46), pp.18109–14.

Zamzami, N. et al., 1996. Inhibitors of permeability transition interfere with the disruption of the mitochondrial transmembrane potential during apoptosis. *FEBS letters*, 384(1), pp.53–7.

Zeng, B. et al., 2011. Developmental patterns and characteristics of epicardial cell markers Tbx18 and Wt1 in murine embryonic heart. *Journal of biomedical science*, 18(1), p.67.

Zhang, F. et al., 2009. VEGF-B is dispensable for blood vessel growth but critical for their survival, and VEGF-B targeting inhibits pathological angiogenesis. *Proceedings of the National Academy of Sciences of the United States of America*, 106(15), pp.6152–7.

Zhou, B. et al., 2011. Adult mouse epicardium modulates myocardial injury by secreting paracrine factors. *The Journal of clinical investigation*, 121(5), pp.1894–904.

Zieba, J. et al., 2015. Behavioural characteristics of the Prader-Willi syndrome related biallelic Snord116 mouse model. *Neuropeptides*, 53, pp.71–7.

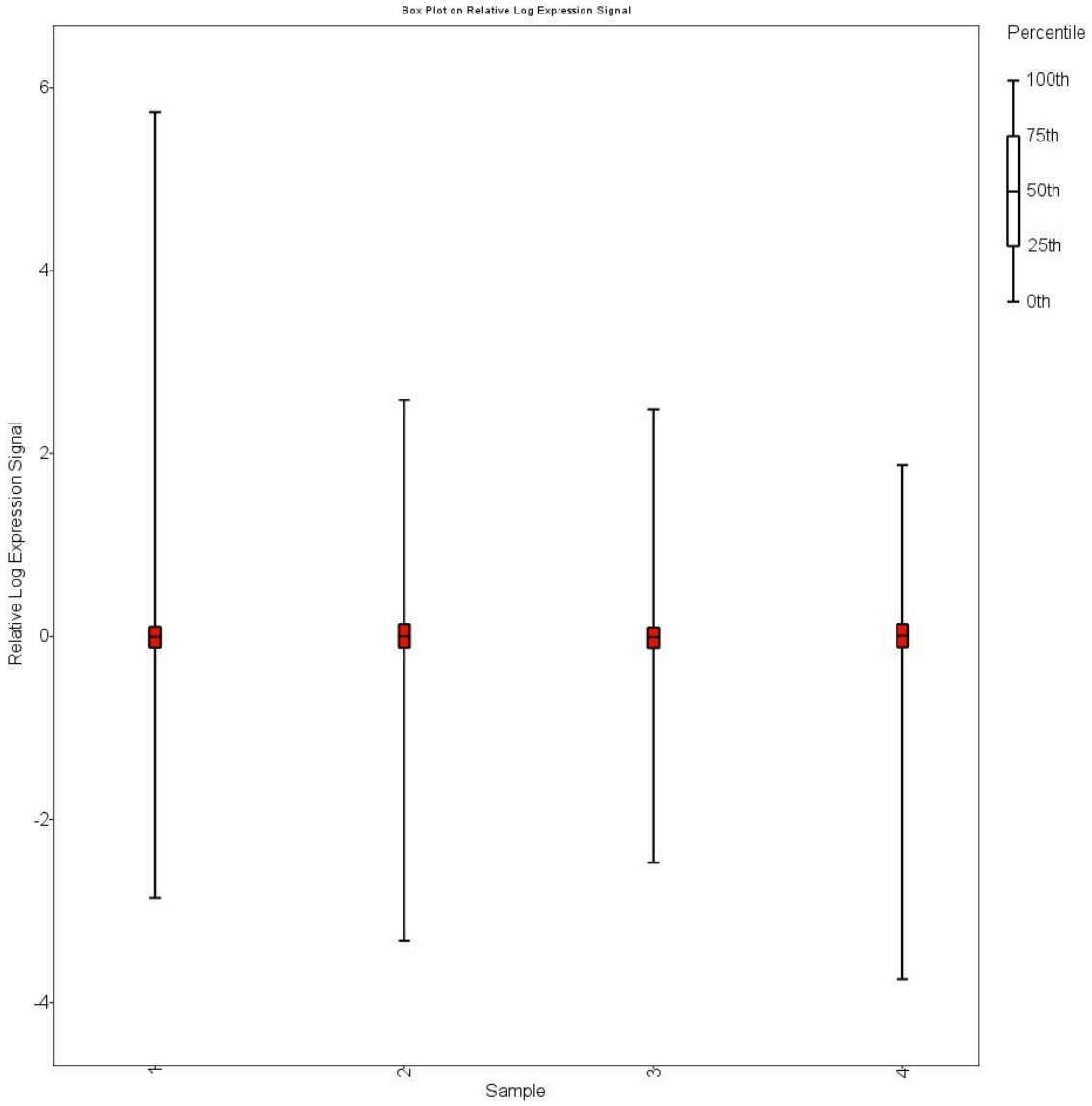

Figure 6. Quality assessment plot for microarray analysis.

.

Appendix 1. Extracellular-matrix related GO term changes (p < 0.05)

Gene Symbol	RefSeq	p-value	Fold-change	Description
Nyx	ENSMUST0000005(	0.000353713	1.07561	R up vs C
Adamts19	NM_175506	0.00485991	-1.2845	R down vs C
Fgfbp3	NM_028263	0.00621279	1.34054	R up vs C
Adamtsl4	ENSMUST00000117	0.00691365	1.11175	R up vs C
Omd	NM_012050	0.0084728	-2.64049	R down vs C
Ltbp4	NM_175641	0.008994	1.14815	R up vs C
Col9a1	NM_007740	0.0129199	1.16006	R up vs C
F2	NM_010168	0.0177218	1.18622	R up vs C
Mmp13	NM_008607	0.0181789	-1.39431	R down vs C
Vit	NM_028813	0.0181927	-1.73122	R down vs C
Col7a1	NM_007738	0.0188026	1.31585	R up vs C
Smoc2	NM_022315	0.0193972	-1.43192	R down vs C
Lad1	NM_133664	0.0221591	1.35419	R up vs C
Mmp3	NM_010809	0.0232333	-1.6688	R down vs C
Crtac1	NM_145123	0.0240654	1.0597	R up vs C
Col1a1	ENSMUST00000001	0.0243705	1.26197	R up vs C
Pkm	NM_011099	0.0262531	1.14644	R up vs C
Mmp19	NM_021412	0.026869	-1.26095	R down vs C
Hpse	NM_152803	0.0274543	-1.20961	R down vs C
Mmp16	ENSMUST00000029	0.030132	-1.10665	R down vs C
Dcn	NM_007833	0.0306457	-1.08987	R down vs C
Impg2	NM_174876	0.0311182	1.18478	R up vs C
Col19a1	NM_007733	0.0315979	1.172	R up vs C
Tnn	NM_177839	0.0344764	1.63442	R up vs C
Gpc5	NM_175500	0.0349341	1.49155	R up vs C
Ptn	NM_008973	0.0350216	-1.59893	R down vs C
Matn2	NM_016762	0.0367851	-1.21501	R down vs C
Ncan	NM_007789	0.0371924	1.51546	R up vs C
Col6a1	ENSMUST00000105	0.0399645	-1.2992	R down vs C
Nav2	NM_175272	0.0423978	1.04991	R up vs C
Wisp1	NM_018865	0.0435078	1.24811	R up vs C
Egfl6	NM_019397	0.0439293	-1.22253	R down vs C
Ogn	NM_008760	0.0457683	-1.40855	R down vs C
Tff3	ENSMUST00000024	0.0479026	1.16069	R up vs C
Adamtsl1	NM_029967	0.0479986	-1.09988	R down vs C

Appendix 2. Nucleic Acid Transcription Factor Binding GO term changes ($p < 0.05$)

Gene Symbol	RefSeq	p-value	Fold-change	Description
Foxg1	NM_001160112	8.45665E-05	1.52685	R up vs C
Cebpz	NM_001024806	0.00028732	-1.19364	R down vs C
Neurod1	ENSMUST0000004	0.000969303	1.2716	R up vs C
Cebpz	NM_001024806	0.00127789	-1.24735	R down vs C
Gm13212	ENSMUST0000010	0.00212063	1.36206	R up vs C
Gm13152	ENSMUST0000006	0.00253476	-1.64509	R down vs C
Gm10324	NM_001177832	0.00287083	2.01704	R up vs C
Zfp260	ENSMUST0000005	0.00318541	-1.29374	R down vs C
Zfp280c	NM_153532	0.00327805	-1.41053	R down vs C
Zfp873	NM_001024626	0.0034278	-1.71725	R down vs C
Nr2f2	NM_183261	0.00494576	1.1682	R up vs C
Pydc3	NM_001162938	0.0051313	1.30067	R up vs C
Nfix	NM_001081982	0.00516407	1.28071	R up vs C
Taf7	NM_175770	0.00531101	-1.54954	R down vs C
Zfp292	NM_013889	0.00552803	-1.20545	R down vs C
Trps1	NM_032000	0.0059242	-1.20386	R down vs C
Hivep2	NM_010437	0.00644032	-1.24902	R down vs C
Tfap4	NM_031182	0.00672151	-1.18639	R down vs C
Nrf1	NM_001164226	0.00677603	-1.27223	R down vs C
Pou2f1	NM_011137	0.00688473	-1.28722	R down vs C
Spen	NM_019763	0.00751398	1.08036	R up vs C
Nfe2l3	NM_010903	0.00763292	-1.18432	R down vs C
Mybl2	ENSMUST0000013	0.00786876	1.31783	R up vs C
Zkscan16	NM_001099323	0.00922455	1.18695	R up vs C
Tbp	ENSMUST0000016	0.0107141	-1.30174	R down vs C
Phox2b	ENSMUST0000001	0.0114535	1.47172	R up vs C
Nr1d2	NM_011584	0.0133043	-1.08283	R down vs C
Pax3	NM_008781	0.0136547	1.28485	R up vs C
Hnf4g	NM_013920	0.015026	1.47782	R up vs C
Nfyb	NM_010914	0.015417	-1.61425	R down vs C
Max	NM_008558	0.0157094	1.0251	R up vs C
Six3	ENSMUST0000016	0.015983	1.25032	R up vs C
Zfp454	ENSMUST0000016	0.0197601	1.41293	R up vs C
Strn3	NM_052973	0.0199519	-1.28384	R down vs C
Tbr1	NM_009322	0.020372	1.04961	R up vs C
Zfp583	NM_001033249	0.0210021	1.09634	R up vs C
Zscan4f	NM_001110316	0.021287	1.3592	R up vs C
Foxa3	NM_008260	0.0214774	1.37347	R up vs C

Gene Symbol	RefSeq	p-value	Fold-change	Description
Rfx1	NM_009055	0.0217291	1.33907	R up vs C
Zfp738	NM_001001187	0.0222254	-1.87227	R down vs C
Zfp26	NM_011753	0.0228167	1.10204	R up vs C
Gm3604	NM_001162910	0.0237986	-2.26011	R down vs C
Tfdp2	NM_178667	0.0244442	-1.13573	R down vs C
Rreb1	NR_033218	0.0256583	1.13678	R up vs C
Rfx8	NM_001145660	0.0269763	1.09434	R up vs C
Myod1	NM_010866	0.0278803	1.32405	R up vs C
Rcor1	ENSMUST0000008	0.0281383	-1.44755	R down vs C
Creb1	NM_133828	0.028558	-1.18364	R down vs C
Zfp708	NM_001012448	0.0293226	-1.9409	R down vs C
Mndal	NM_001170853	0.029535	-1.70056	R down vs C
Barhl2	ENSMUST0000008	0.0299535	1.12684	R up vs C
Sox4	ENSMUST0000006	0.0303399	-1.21826	R down vs C
Zfp758	NM_145484	0.0329337	-1.77883	R down vs C
Trp63	NM_001127259	0.0331425	1.21736	R up vs C
Smad2	NM_001252481	0.033868	-1.1869	R down vs C
Onecut2	NM_194268	0.0340372	1.50857	R up vs C
Klf17	NM_029416	0.0345984	1.17917	R up vs C
Pyhin1	NM_175026	0.036212	-2.46849	R down vs C
Foxs1	NM_010226	0.0366845	-1.37471	R down vs C
Hoxa3	ENSMUST0000011	0.0373524	1.44064	R up vs C
Mef2b	NM_008578	0.0373947	1.4804	R up vs C
C030039L03Rik	NM_198417	0.039011	1.41853	R up vs C
Foxd4	NM_008022	0.0395271	1.17199	R up vs C
E2f2	NM_177733	0.0400394	1.61577	R up vs C
Zfp954	NM_172738	0.0403186	-1.88372	R down vs C
Myt1l	NM_001093775	0.0403235	1.39268	R up vs C
Gm14431	NM_001177406	0.0406031	-1.25388	R down vs C
Zfp72	NM_001081680	0.0409253	-1.25103	R down vs C
Sp4	NM_009239	0.0409446	-1.426	R down vs C
Msgn1	NM_019544	0.0415572	1.65395	R up vs C
Zfp280d	BC027163	0.0422592	-1.16838	R down vs C
Gpbp1	ENSMUST0000004	0.0428043	-1.41416	R down vs C
Sall4	NM_175303	0.042807	1.47252	R up vs C
E2f5	NM_007892	0.0433716	-1.16136	R down vs C
Zfx	NM_001044386	0.0439853	-1.29493	R down vs C
Dmrtc2	NM_027732	0.0443115	1.3555	R up vs C
2410141K09Rik	NM_183119	0.0443612	1.65326	R up vs C
Bhlha15	NM_010800	0.0451731	1.47976	R up vs C
Klf7	ENSMUST0000011	0.045181	-1.58596	R down vs C
Myocd	NM_145136	0.0464727	1.24754	R up vs C
Zfp420	NM_172740	0.0484832	-1.46786	R down vs C
Zfp174	NM_001081217	0.0487177	1.39146	R up vs C
Tfap2a	NM_011547	0.0498445	1.22812	R up vs C

Appendix 3. Reproductive GO term changes ($p < 0.05$)

Gene Symbol	RefSeq	p-value	Fold-change	Description
Bcl2	NM_009741	0.000337	-1.26863	R down vs C
Spin4	NM_178753	0.00045	-1.35393	R down vs C
Prdx4	NM_016764	0.000473	-1.61472	R down vs C
Ddx4	NM_001145885	0.000878	1.23375	R up vs C
Immp2l	ENSMUST000001	0.001299	-1.40526	R down vs C
Lrp6	NM_008514	0.001843	1.12648	R up vs C
Atp8b3	NM_026094	0.00206	1.20365	R up vs C
Syce1	NM_001143765	0.002348	1.1989	R up vs C
Cul7	NM_025611	0.002531	1.19327	R up vs C
Nr2f2	NM_183261	0.004946	1.1682	R up vs C
Meig1	ENSMUST000001	0.005948	-1.6268	R down vs C
Jag2	NM_010588	0.006431	1.11351	R up vs C
Th	ENSMUST000000	0.007041	1.21415	R up vs C
Map2k1	NM_008927	0.007998	-1.16327	R down vs C
Birc6	NM_007566	0.00851	-1.11453	R down vs C
Plekha1	NM_133942	0.009155	-1.24818	R down vs C
Corin	NM_016869	0.010197	1.20051	R up vs C
Ift81	NM_009879	0.010946	-1.61298	R down vs C
Angpt1	ENSMUST000000	0.0113	-1.84062	R down vs C
Dicer1	NM_148948	0.011597	-1.20149	R down vs C
Cdh1	NM_009864	0.011853	-1.22617	R down vs C
Exo1	NM_012012	0.011946	1.54586	R up vs C
Atm	NM_007499	0.01197	-1.41555	R down vs C
Zfp37	NM_009554	0.013281	1.09552	R up vs C
Rad23b	NM_009011	0.013461	-1.13956	R down vs C
Fancl	ENSMUST000000	0.01347	-1.47642	R down vs C
Smc3	NM_007790	0.013632	-1.17291	R down vs C
Rps6	NM_009096	0.014052	-1.03026	R down vs C
Rad21l	NM_001114677	0.014082	1.21252	R up vs C
Kitl	ENSMUST000001	0.014372	-1.24251	R down vs C
Tle3	NM_001083927	0.014802	1.12531	R up vs C
Tiparp	NM_178892	0.015107	-1.56611	R down vs C
Stk3	NM_019635	0.015633	-1.42692	R down vs C
Dld	NM_007861	0.015677	-1.351	R down vs C
Golga3	ENSMUST000001	0.015776	-1.28204	R down vs C
Bptf	NM_176850	0.016261	-1.09183	R down vs C
Lgr5	NM_010195	0.016527	-1.2999	R down vs C
Src	ENSMUST000001	0.017835	-1.18975	R down vs C
Aurka	NM_011497	0.017905	1.48953	R up vs C
Rnase9	NM_183032	0.018282	1.29313	R up vs C
Mir34b	NR_029655	0.018371	1.76618	R up vs C
Chd7	ENSMUST000000	0.018425	-1.13204	R down vs C
Magoh	ENSMUST000000	0.018967	-1.38423	R down vs C
Ttc26	ENSMUST000001	0.019519	-1.24241	R down vs C
Ift88	NM_009376	0.019866	-1.21459	R down vs C
Stag3	NM_016964	0.020232	1.59994	R up vs C
Foxa3	NM_008260	0.021477	1.37347	R up vs C
Plk1	NM_011121	0.021584	1.34933	R up vs C

Gene Symbol	RefSeq	p-value	Fold-change	Description
Tubd1	NM_001199045	0.022088	-1.47585	R down vs C
Gm16405	NM_001166646	0.022274	1.62965	R up vs C
Sos1	NM_009231	0.023653	-1.15704	R down vs C
Gm16405	NM_001166646	0.024036	1.63986	R up vs C
Tial1	ENSMUST000001	0.024081	-1.2188	R down vs C
Spata18	ENSMUST000000	0.024163	1.29712	R up vs C
Mlh3	NM_175337	0.024182	-1.52851	R down vs C
Mnd1	NM_029797	0.02553	-1.71702	R down vs C
Larp7	NM_138593	0.025623	-1.24027	R down vs C
Top2a	NM_011623	0.025679	1.26988	R up vs C
Dnajb6	ENSMUST000000	0.026432	-1.1576	R down vs C
Ggn	NM_182694	0.0273	1.19814	R up vs C
Mir449c	NR_030452	0.028143	1.38545	R up vs C
Mlh1	NM_026810	0.02847	-1.22918	R down vs C
Strbp	NM_009261	0.028915	-1.20595	R down vs C
Fzd5	NM_022721	0.028933	1.04561	R up vs C
Spaca3	ENSMUST000001	0.029877	1.24536	R up vs C
Edn2	ENSMUST000000	0.030225	1.12367	R up vs C
Tdrd7	ENSMUST000001	0.030642	-1.21717	R down vs C
Adam26a	NM_010085	0.030944	1.14646	R up vs C
Ror2	NM_013846	0.031222	1.29694	R up vs C
Racgap1	NM_012025	0.031762	1.349	R up vs C
Tbata	NM_001017433	0.032369	1.31109	R up vs C
Spin1	NM_011462	0.033071	-1.27487	R down vs C
Trp63	NM_001127259	0.033143	1.21736	R up vs C
Gm16405	NM_001166646	0.034552	1.56139	R up vs C
Klf17	NM_029416	0.034598	1.17917	R up vs C
Rbm7	NR_037589	0.034704	-1.355	R down vs C
Arid4a	NM_001081195	0.034786	-1.25435	R down vs C
Prss29	NM_053260	0.035283	1.32047	R up vs C
Bmpr1b	NM_007560	0.035595	-1.41594	R down vs C
Senp2	NR_027488	0.035667	-1.36295	R down vs C
Tcp1	ENSMUST000001	0.036353	-1.36122	R down vs C
Xlr5b	ENSMUST000001	0.036592	1.25332	R up vs C
Ccdc155	ENSMUST000001	0.036816	1.2357	R up vs C
Xlr5a	NM_001045539	0.038287	1.34647	R up vs C
Insl6	NM_013754	0.038308	-1.36024	R down vs C
Mastl	ENSMUST000000	0.038891	-1.24928	R down vs C
Zpbp	ENSMUST000000	0.039527	-1.22044	R down vs C
Nme5	NM_080637	0.039912	-1.98329	R down vs C
Nrip1	ENSMUST000001	0.040525	-1.14789	R down vs C
3830403N18Rik	NM_027510	0.041356	-1.5917	R down vs C
Ggt1	ENSMUST000000	0.041362	1.24216	R up vs C
Ube2a	NM_019668	0.042862	-1.43152	R down vs C
Zfx	NM_001044386	0.043985	-1.29493	R down vs C
Xlr3b	NM_001081643	0.044181	-3.1188	R down vs C
Dmrtc2	NM_027732	0.044312	1.3555	R up vs C
Gm16405	NM_001166646	0.046434	1.52703	R up vs C
Myocd	NM_145136	0.046473	1.24754	R up vs C

Gene Symbol	RefSeq	p-value	Fold-change	Description
Klhdc3	NM_027910	0.046614	-1.22938	R down vs C
Sly	NM_201530	0.047469	3.1055	R up vs C
Sly	NM_201530	0.047469	3.1055	R up vs C
Plcb1	NM_001145830	0.047543	-1.22738	R down vs C
Syna	NM_001013751	0.047634	1.21241	R up vs C
Ubr2	NM_146078	0.048423	-1.1173	R down vs C
Tmf1	NM_001081111	0.048762	-1.29388	R down vs C
Pank2	NM_153501	0.048945	-1.32359	R down vs C
Gm16405	NM_001166646	0.049326	1.56571	R up vs C
Gm16405	NM_001166646	0.049326	1.56571	R up vs C
Ada	ENSMUST000000	0.049698	-1.10595	R down vs C
Rpa1	NM_001164223	0.049822	-1.18088	R down vs C
Cr1l	NM_013499	0.049854	-1.21465	R down vs C